UNDERSTANDING THE ROLE OF DNA LIGASES IN CHRONIC LYMPHOCYTIC LEUKEMIA

Thesis submitted in accordance with the requirements of

the University of Liverpool for the degree of

Master of Philosophy

by

Sanghamitra Vundyala

September 2016

Contents

Contents ..... **i**

Abstract ..... **i**

List of Figures ..... **iii**

List of Tables ..... **v**

Acknowledgement ..... **vi**

Declaration ..... **vii**

Abbreviations ..... **viii**

Chapter 1: Introduction **1**

1.1 Sources of DNA damage 1
1.2 DNA Repair Mechanisms 2
1.2.1 Base Excision Repair (BER) 4
1.2.2 Nucleotide Excision Repair (NER) 4
1.2.3 Mismatch Repair (MMR) 5
1.2.4 Homologous Recombination (HR) 6
1.3 VDJ Recombination 7
1.4 DNA Ligases 9
1.4.1 DNA Ligase1 9
1.4.2 DNA Ligase 3 12
1.4.3 DNA Ligase 4 12
1.5 Non Homologous End Joining (NHEJ) 15
1.6 Other proteins involved in NHEJ pathway 16
1.6.1 Ku70/80 16
1.6.2 DNA-PKcs 18
1.6.3 Artemis 19
1.6.4 X-ray Repair Cross Complementing Protein (XRCC4) 20
1.6.5 XRCC4 Like Factor (XLF) 22
1.6.6 DNA Polymerases 23
1.6.7 NHEJ pathway 23
1.6.8 NHEJ and its role in Cancer 24
1.6.9 Synthetic inhibitors of NHEJ 28
1.7 Chronic Lymphocytic Leukaemia 30
1.7.1 DNA damage in CLL 32

Aims **34**

Chapter 2: Methods 35

2.1 Cell culture 35
2.1.1 Cell line culture and maintenance 35
2.1.2 Cell thawing 35
2.1.3 Cell line passaging 36
2.1.4 Cell line freezing 36
2.2 Molecular Biology 37
2.2.1 RNA extraction 37
2.2.2 cDNA synthesis protocol 39
2.2.3 Polymerase chain reaction (PCR) 39
2.2.4 Agarose gel electrophoresis 40
2.3 Protein analysis 41
2.3.1 Cell lysis and protein determination 41
2.3.2 Western blotting 42
2.4 Measurement of cell proliferation using a colorimetric BrdU ELISA assay 44
2.5 Measuring apoptosis of cells by flow cytometry using PI and DiOC6 46
2.5.1 Measuring apoptosis of cells upon treatment with irradiation only 47
2.5.2 Measuring cytotoxicity and radiosensitivity of cells upon treatment with different concentrations of SCR7 inhibitor and irradiation 47
2.6 Statistical analysis 48

Chapter 3: Results 49

3.1 Verifying cDNA quality using *GAPDH* primers 49
3.2 Optimisation of annealing temperature of primers specific for DNA ligases 50
3.3 Determination of the expression of *LIG4, LIG3* and *LIG1* mRNA in CLL samples and the human bone marrow stromal cell line (HS-5) 54
3.4 Analysis of DNA Ligase 4 protein expression in haematopoietic cell lines 55
3.5 Analysis of the expression of Ligase 4 and XRCC4 proteins in CLL patient samples 58
3.6 Analysis of the effects of irradiation on expression of Ligase 4, XRCC4 and p53 proteins 58
3.7 Analysis of the effects of irradiation and SCR7 on growth and survival in haematopoietic cell lines 62
3.8 Analysis of the sensitivity of leukemic cells to irradiation following pre-treatment with SCR7 inhibitor 65
3.9 Investigation of effects on cell proliferation upon treatment with SCR7 inhibitor and irradiation 67

Chapter 4: Discussion.....72

Appendix 81

References 83

Abstract

DNA ligases ascertain and facilitate genomic integrity by ensuring DNA repair during synthesis and replication. One of the most lethal forms of DNA damage is a double strand break which can lead to loss of more than 100 million base pairs of genetic information. The Non Homologous End Joining (NHEJ) DNA repair pathway is sequence independent and involves recruitment of several proteins such as Ku70/80, Artemis, DNA-$PK_{cs,}$ Ligase 4 and XRCC4 for ligation and repair of the broken double strand DNA ends. Evidence in the literature suggests that some of the key players in the NHEJ pathway have distinct roles in cancer and in addition contribute to development of resistance to chemo-radiotherapy.

Several studies indicate that disruption of the *LIG4* gene(DNA ligase 4) - a critical component of the NHEJ pathway, results in increased sensitivity of cells to ionizing irradiation. In this study we have explored the relevance DNA Ligase 4 in Chronic Lymphocytic Leukemia (CLL). Using endpoint PCR analysis we detect the expression of *LIG1, LIG3 and LIG4* genes in a small cohort of primary CLL cases. Protein expression of Ligase 4 was detected in HeLa (positive control), MEC1 (a CLL line) cells and in a random cohort of CLL cases. Surprisingly, Ligase 4 and XRCC4 protein expression did not alter in response to irradiation (3 Gy and 5 Gy) in MEC1 or HeLa cells.

SCR7, a specific inhibitor of Ligase 4, was used to study cell cytotoxicity in response to irradiation. Both MEC1 and Daudi cells showed increased cell death upon treatment with high concentrations (250 µM) of the drug alone. Radiosensitivity experiments using SCR7

(10 µM and 100 µM) treatment prior to irradiation of cells showed no significant change in cell death in both MEC1 cells and Daudi cells at sequential time points. Although the results generated during this study provide some insights into the expression of certain DNA repair components in CLL, a longer and more substantive study in a larger cohort of patient samples is required for more definitive conclusions to address the relevance in CLL.

List of Figures

Figure 1: Pictorial representation of various DNA Damaging agents generating a wide variety of DNA lesions including SSBs, DSBs, insertions and deletions which require or trigger repair machinery.....3

Figure 2: Representation of DNA Ligase reaction mechanism 10

Figure 3: Structure of human DNA Ligase 1 polypeptide.....11

Figure 4 : Structure of human DNA Ligase 3 polypeptides.....13

Figure 5: The domain model of Ligase 4 protein. 15

Figure 6: Typical three dimesional structure reconstruction of a Ku70/80 heterodimer using images from electron microscopy 17

Figure 7: Structural representation of Ku heterodimers 17

Figure 8: The structure of DNA-PK_{cs}. 19

Figure 9: The domain architecture of artemis protein 20

Figure 10: XRCC4 domain architecture.....21

Figure 11: Domain structure of XLF protein.....34

Figure 12: Mechanism of DSB repair by NHEJ pathway 25

Figure 13: Structure showing interactions between DNA binding domain of Ligase 4 protein and SCR7 inhibitor.. 43

Figure 14: Verifying cDNA quality using *GAPDH* primers.....49

Figure 15: Gradient PCR of primer sets to determine optimal annealing temperature 51

Figure 16: End point PCR using *LIG4* primer set 4 and cDNA extracted from primary CLL patient samples.....54

Figure 17: Endpoint PCR of *LIG3* and *LIG1* using described primer sets with cDNA extracted from CLL patient samples.....54

Figure 18: Western blot depicting Ligase 4 protein expression in a panel of lymphoid cell lines using a Ligase 4 antibody (Protein Tech, UK) 55

Figure 19: Western blot analysis of DNA Ligase 4 protein expression in cell lines using an Anti-DNA Ligase IV antibody (Abcam, UK) 56

Figure 20: Western blot analysis of downstream NHEJ proteins in a variety of cell lines ..... **Error! Bookmark not defined.**

Figure 21: Verifying the protein expression of Ligase 4 and XRCC4 in CLL cases 60

Figure 23: Effect of IR (3 Gy and 5 Gy) after 24, 48 and 72 hours on DNA Ligase 4, XRCC4 and p53 expression in HeLa and MEC1 cells 61

Figure 24: Assessment of cytoxicity in Daudi cells on treatment with irradition and/or SCR7 63

Figure 25: Assessment of cytotoxicity in MEC1 cells following exposure to irradiation and/or SCR7. 64

Figure 26: Assessment of radiosensitivity assay of Daudi cells on pre-treatment with SCR7. 66

Figure 27: Assessment of radiosensitivity of MEC1 cells pre-treated with SCR7 67

Figure 28: BrdU assay to assess cell proliferation of HeLa cells subjected to IR and SCR7 inhibitor.....69

Figure 29: BrdU assay measuring cell proliferation of MEC1 cells upon subjection to IR and SCR7 inhibitor.....70

Figure 30: BrdU assay measuring cell proliferation of Daudi cells upon exposure to IR and SCR7 inhibitor 71

List of Tables

Table 1: List of cell lines used and culture method. 37

Table 2: The above table comprises of the list of antibodies and their respective final dilutions used for studying protein expression. 44

Table 3: Characteristics of primers used for PCR amplification of *LIG1*, *3* and *4* genes along with *GAPDH* primers 53

Table 4 : The list of primers used in the next set of experiments. 53

Table 5: Percentage of dead cells in MEC1 and Daudi cell lines under various treatment conditions with SCR7 and 5 Gy IR. 64

Table 6: Clinical data of all the CLL patients used in the project. 81

Table 7: Raw data of radiosensitivity assay 81

Table 8: Raw data values of cytotoxicity assays for Daudi and MEC1 cells at 24 , 48 and 72 hours 82

Acknowledgement

Firstly I would like to convey my sincere gratitude to my project supervisors Dr. Nagesh Kalakonda and Dr. Joseph Slupsky for their immense support and able guidance throughout the project. I would also like to thank Dr. Mark Glenn and Dr. Jemma Blocksidge for their constant help with my lab work, thesis writing, and answering all my questions patiently. I would like to thank my lab colleagues for their continual help, Dr. Alix Bee for helping me with irradiation of my samples, Dr. Ola Al-Sanabra and Dr. Mosavar Farahani (a special mention to Mr. Venkateswarlu Perikala) for providing me with cDNA samples and protein lysates. I wish to thank Dr. Sathees Raghavan for providing us with the SCR7 inhibitor for my project. Last but not least, I wish to thank my parents, my husband Pavan, my sister Sahitya, my family and friends for their constant encouragement, support and their belief in me.

Declaration

All practical laboratory work, was carried out in the Cancer Biology laboratory of Dr. Nagesh Kalakonda, Department of Molecular and Clinical Cancer Medicine, Institute of Translational Medicine, University of Liverpool.

The usage of the Flow cytometry equipment was supervised by Dr. Mark Glenn. The work presented in this thesis is my own.

Abbreviations

AdD: Adenylation domain

AMP: Adenosine mono phosphate

AP: Apurinic/Apyrimidinic sites

APE1: AP endonuclease

APS: Ammonium per sulphate

ATAD5: ATPase Family, AAA Domain Containing 5

ATM: Ataxia Telangiectasia Mutated

ATP: Adenosine tri phosphate

ATR: Ataxia Telangiectasia and Rad3 related protein

BCR: B cell antigen receptor

BER: Base excision repair

BRCT: BRCA1 C terminus domain

BRDU: Bromodeoxyuridine

CHK1: Checkpoint Kinase 1

CHK2: Checkpoint Kinase 1

CO_2: Carbon dioxide

CSA: Cockayne syndrome group A gene

CSB: Cockayne syndrome group B gene

CT: Carboxy-terminal region

DBD: DNA binding domain

DDB1: DNA damage-binding protein 1

DDB2: DNA damage-binding protein 2

DNA: Deoxyribonucleic acid

DNA-PK_{cs}: DNA-dependent protein kinase, catalytic subunit

dRP: 2-Deoxyribose phosphodiesterase

DSB: Double stranded breaks

DTT: Dithiothreitol

EDTA: Ethylenediaminetetraacetic acid

EGFR: Epidermal growth factor receptor

FAT: Focal adhesion targeting domain

g: gravitational force

GGR: Global genomic repair

Gy: Gray

HR: Homologous recombination

IR: Ionising radiation

Lig1: DNA ligase 1 enzyme

LIG1: DNA Ligase 1 gene

Lig3: DNA ligase 3 enzyme

LIG3: DNA Ligase 3 gene

Lig4: DNA ligase 4 enzyme

LIG4: DNA Ligase 4 gene

LRR: Leucine rich region

mg: milligram

mL: millilitre

MLS: Mitochondrial leader sequence

MMR: Mismatch repair

mRNA: mRNA

MSH2: MutS Homolog 2

MSH3: MutS Homolog3

MSH6: MutS Homolog6

NER: Nucletide excision repair

NFW: Nuclease free water

ng: Nanogram

NHEJ: Non homologous end joining

NLS: Nuclear localization sequence

Nm: Nanometer

OBD: Oligo binding domain

PAGE: Polyacrylamide gel electrophoresis

PB: Peripheral blood

PBS: Phosphate-buffered saline

PCC: Post cleavage complex

PI3K: Phosphoinositide 3-kinase

PMS2: Post meiotic segregation increased 2

Polδ: Polymerase delta

Polε: Polymerase epsilon

PRD: Phosphoinositide 3-kinase regulatory domain

PVDF: Polyvinylidene fluoride

RFTS: Replication factory targeting sequence

RNA: Ribonucleic acid

RPA: Replication protein A

RSS: Recombination signal sequence

SAP: SAF-A/B, Acinus and PIAS domain

SCID: Severe combinded immunodefieciency

SDS: Sodium dodecyl sulphate

SSB: Single stranded breaks

TBE: Tris/Borate/EDTA

TBS: Tris buffered saline

TCR: T cell antigen receptor

TCR: Transcription-coupled repair

TEMED: Tetramethylethylenediamine

TFIIH:Transcription factor II Human

UV: Ultra violet

V: Volts

vWA: von Willibrand A domain

XLF: XRCC4 like factor

XPA: Xeroderma pigmentosum complementation group A

XPC-HR23B: Xeroderma pigmentosum complementation group C protein complex

XRCC2: X-ray repair cross complementing protein 2

XRCC3: X-ray repair cross complementing protein 3

XRCC4: X-ray repair cross complementing protein 4

µg: Microgram

µL: Microlitre

µm: Micromolar

Chapter 1: Introduction

Keeping our genome intact is vital for faithful transfer of genetic information from one generation to another, as our genome is subjected to several external and endogenous insults, which cause damage of Deoxyribonucleic acid (DNA) resulting in harmful mutations and diseases including cancer[1].

1.1 Sources of DNA damage

DNA damage is mainly caused by environmental factors such as ultraviolet (UV) rays, ionising radiation (IR), genotoxic substances (for example, those present in cigarettes) and alkylating agents. These agents cause aberrations in the DNA sequence producing both Single Strand Breaks (SSB) and Double Strand Breaks (DSB)[2]. IR can damage DNA directly and indirectly. In most instances the radiation energy is directly absorbed by the DNA resulting in ionisation and breakage of the DNA strand[3]. As the majority of biological systems are made of water, the by-products released on irradiation of water are indirect sources of DNA damage. Radiolysis of water produces reactive species such as hydroxyl radicals (superoxide and peroxide radicals), which attack the DNA bases and sugars and form a wide variety of lesions, mainly DSBs[2,4,5]. A DSB is produced when two or

more hydroxyl radicals attack both the strands of DNA. In a typical reaction of IR with DNA, initially, a water molecule is ionised due to high ionising energy. The water molecule loses a proton to generate a hydroxyl radical (• HO). The activated electron reacts further with oxygen to produce a superoxide radical (O_2•). There are reported incidences of the hydroxyl radical attacking one strand of the DNA and then getting transported to the next strand to cause damage as electronic charges generated from IR can travel through long distances across the DNA helix[2,6]. Secondly, cellular metabolism results in fragmentation, base loss, and SSBs of DNA due to the release of reactive oxygen species (ROS) such as hydroxyl radicals; superoxide anions and hydrogen peroxide, thereby causing oxidative damage[7]. In addition, spontaneous decay of the primary structure of DNA under certain conditions such as DNA hydrolysis, DNA oxidation and non-enzymatic methylation of DNA, gives rise to DNA breakage[8]. Replication errors during DNA synthesis are also responsible for causing nucleotide mismatches in DNA during the S phase of the cell cycle, resulting in the generation of insertions and deletions in the DNA helix[9].

1.2 DNA Repair Mechanisms

There are several different DNA repair mechanism systems in

mammals which are triggered in response to the type of DNA damage. They are: Base Excision Repair (BER), Nucleotide Excision Repair (NER), Mismatch Repair (MMR), Homologous Recombination (HR) and Non Homologous End Joining (NHEJ) (**Fig 1**).

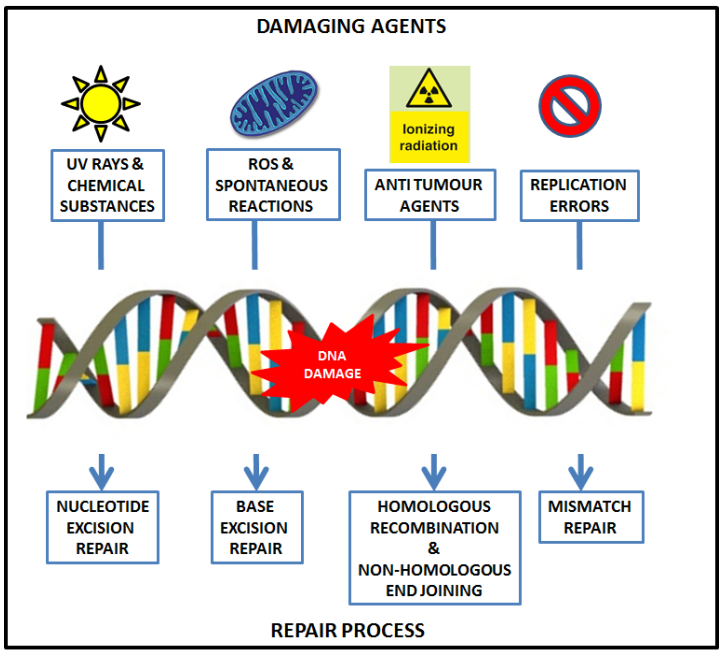

Figure 1: Pictorial representation of various DNA Damaging agents generating a wide variety of DNA lesions including SSBs, DSBs, insertions and deletions which require or trigger repair machinery (adapted from Hoejimakers JH *et al.,* 2001) [1].

DNA damage in the form of SSBs, mismatched bases, insertions, deletions, and addition of bulky adducts is repaired by BER, NER and MMR. In contrast, the two main pathways that have evolved to counter DSBs generated inadvertently are HR and NHEJ[2].

1.2.1 Base Excision Repair (BER)

Many of the DNA lesions in the form of SSBs and abasic sites which are repaired by BER, are formed by oxidative stress, alkylating agents and spontaneous reactions of DNA[2,10]. In BER, the damaged base is excised using the DNA glycosylases, which help in removing the chemically altered base from DNA by hydrolysing the N-glycosidic bonds[11]. To further remove the abasic, apurinic or apyrimidinic sites (AP), the apurinic or apyridimidinic endonucleases are recruited on the AP site; in mammals, AP endonuclease (APE1) is the most commonly recruited endonuclease. The AP sites are incised by APE1 endonuclease which cuts through the phospho- backbone of DNA[12]. After excising the abasic site, other enzymes including 2-deoxyribose phosphodiesterase (dRP), DNA polymerase, DNA Ligase 1 and DNA Ligase 3 assist in the synthesis and repair[10]. There are two different types of BER pathways; one is the ‘short patch repair’ that helps in the replacement of a single nucleotide, whereas, the ‘long patch repair’ helps in the replacement of a series of nucleotides[13].

1.2.2 Nucleotide Excision Repair (NER)

NER is responsible for the repair of bulky DNA lesions produced as a result of genotoxic chemicals and UV light. NER operates via two distinct pathways: Global Genomic Repair (GGR) and Transcription-Coupled Repair (TCR)[14]. GGR is transcription independent and

removes DNA adducts from the non-transcribed portions of the genome, whereas, TCR repairs transcription-hindering lesions of DNA[15]. Approximately 30 proteins are involved for successful completion of NER, with the essential ones being: Xeroderma Pigmentosum Complementation group C protein complex (XPC-HR23B), Xeroderma Pigmentosum Complementation group A (XPA), Replication Protein A (RPA), DNA Damage-Binding protein 1 (DDB1), DNA Damage-Binding protein 2 (DDB2), Transcription Factor II Human (TFIIH) and Cockayne syndrome group A and B genes (CSA and CSB). XPC-HR23B aids in identifying the lesions in GGR, whereas in TCR, Ribonucleicacid polymerase II helps in identifying the damaged area. TFIIH is recruited in the next step in both of the processes, to open up the DNA helix around the lesion. Other cofactors, namely CSA and CSB are recruited to make the lesion more accessible to the next set of repair proteins[16]. XPA stabilises the opened helix around the lesion and the RPA protein's major function is to safeguard the intact DNA strand[17,18]. During both repair mechanisms, the DNA is resynthesised by Polymerase epsilon(Polε) or Polymerase delta(Polδ) and re-ligation is performed by Ligase 1[10,19].

1.2.3 Mismatch Repair (MMR)

MMR plays a major role in eukaryotic cells to correct and prevent mutations caused by mismatch of bases during replication of DNA[2].

Replication errors are one of the main sources of mismatches, leading to the formation of insertions and deletions of nucleotides in the DNA sequence. Other sources include spontaneous decay of DNA due to base deamination, oxidation and methylation[20,21]. The DNA mismatches are repaired by a specific set of proteins: MutS Homolog 2 (MSH2), MutS Homolog 6 (MSH6), MutS Homolog 3 (MSH3), MutL Homolog 1 (MLH1) and Post Meiotic Segregation increased 2 (PMS2) belonging to the MutS and MutL families[22]. MSH2 and MSH6 together form the MutSα complex, which repairs single base mismatches; MSH2 and MSH3 form the MutSβ complex that repairs longer mismatched nucleotides[23]. Exo I assists in excising the mismatched base on the 3' strand with the help of MutS and MutL proteins, whereas for excising a mismatched base on the 5' strand only MutS proteins are required. Ligase 3 and Polδ are involved in re-synthesising the DNA and sealing the gap caused by the excision[24,25].

1.2.4 Homologous Recombination (HR)

Homology directed repair is an error free, template dependent process, which helps in accurately re-synthesising the damaged DNA at the break site[26]. HR occurs in late S and G2 phases of the cell cycle[27]. In HR, the DNA with the DSB seeks an undamaged homologous DNA strand to use as a template molecule for repair. The first step of HR involves trimming back of one strand of DNA in 5' to 3'

direction by the MRE11–Rad50–NBS1 complex, leading to the formation of a 3’ single-stranded DNA fragment[28]. The Rad52 nucleoprotein binds to this fragment and interacts with Rad51 causing an interchange with the undamaged DNA strand[29]. RPA assists Rad51 protein in the formation of nucleoprotein filaments which adhere to undamaged DNA with the help of its sister proteins Rad51B, Rad51C and Rad51D, X-ray repair cross complementing protein2 (XRCC2) and X-ray repair cross complementing protein3 (XRCC3)[30-32]. The DNA strand interchange between homologous duplexes leads to the formation of Holliday junctions resulting in heteroduplex DNA formation with four junctions which migrates along the DNA and increases the length of the heteroduplex DNA. This phenomenon is known as branch migration[33]. The Holliday junctions are initiated by a class of enzymes known as the resolvases. Only two eukaryotic resolvases have been identified so far; Yen1 resolvase in yeast and GEN1 resolvase in humans[34,35]. After the homology search and strand invasion, the damaged DNA is extended by polymerases generating two intact DNA fragments and Ligase 1 rejoins the broken ends[36,37].

1.3 VDJ Recombination

VDJ recombination is a critical step during B and T cell differentiation in which these cells undergo recombination to generate a wide array of B and T cell antigen receptors (BCR & TCR)[38]. In mammals there are

seven antigen receptor loci, which vary in configuration and the number of Variation (V), Diversity (D) and Joining (J) segments. A typical germ line antigen locus contains V, D, J segments along with a recombination signal sequence (RSS) made up of heptamer and nonamer elements. VDJ recombinase is an enzyme made up of recombination activating genes 1 and 2 (RAG1 & RAG2), which cleave at the RSS sequence causing a single strand nick between RSS sequence and the adjacent coding segment[39]. The nicking results in the generation of 3' OH group, which uses another RSS sequence by binding to it, thereby creating a DSB. This interaction produces broken ends of DNA in the form of two hairpin ends and 2 blunt ends. These broken DNA ends, continue their linkage with RAG proteins forming the post cleavage complex (PCC)[40]. The RAG proteins are a part of PCC, they direct the broken ends to enter the NHEJ pathway, thereby producing rearranged gene segments known as coding joint and signal joint[41]. The coding joint comprises of V-DJ for heavy chains and V-J for light chains, whereas the signal joint consists of head to head linkage of RSS sequences. At times, the repair of the breaks formed in VDJ recombination becomes deviant leading to formationof chromosomal translocations, inversions and deletions. Such consequences lead to genomic instability resulting in lymphoid malignancies. This feature is commonly observed in Leukemias.

1.4 DNA Ligases

Mammalian DNA ligases belong to a family of phosphotransferase enzymes known nucleotidyltransferases that use adenosine triphosphate (ATP) as a cofactor[42]. They are involved in the formation of phosphodiester bonds between neighbouring 3' hydroxyl and 5' phosphate groups in nicked DNA [43]. All the three DNA ligase enzymes, *Lig1, 3* and *4*, share a similar catalytic core comprising of an OBD and AdD domains. An additional DBD boosts the activity of the catalytic region. The mechanism of DNA ligases functioning has been explained in (**Fig 2**).

1.4.1 DNA Ligase1

The human DNA *LIG1* gene encodes the single Ligase 1 polypeptide. Ligase 1 polypeptide is made up of 919 amino acids (**Fig 3**). The structure of polypeptide is mainly composed of a non-catalytic core consisting of a nuclear localization signal (NLS) and replication factory targeting sequence (RFTS). The conserved catalytic core consists of the OBD, AdD and DBD domains[44]. The Ligase 1 enzyme is known to be an active participant in DNA replication [45]. The catalytic core of Ligase 1 is involved in the ligation of DNA nicks between nearby Okazaki fragments (shorter DNA fragments created anew on the lagging strand during DNA replication), that are made up of 150-200 nucleotides[46]. One of the proteins known to interact with Ligase 1

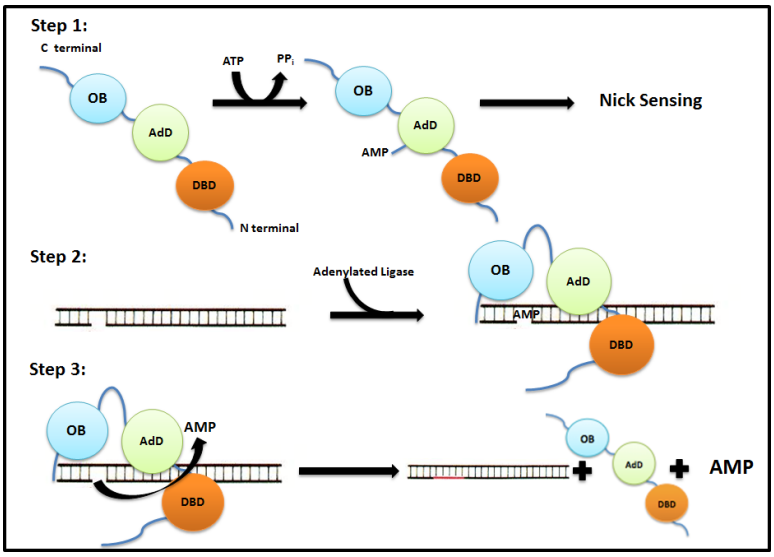

Figure 2: Representation of DNA Ligase reaction mechanism.

The catalytic region of DNA ligases consists of OB(Oligobinding domain) AdD(Adenylation domain) and DBD (DNA binding domain) domains.The catalytic regions interacts with ATP to release a pyrophosphate. When an adenylated ligase recognises a nick and binds to it, it undergoes a confirmational change such that all the ligase encircles the nick.The AMP from AdD attaches itself to the 5' phosphate group of the nick. The non adenylated ligase now uses the 3' hydroxyl group as a nucleophile to attack the 5' adenylate resulting in phosphodiester bond formation and release of Ligase and AMP(adapted from Tomkinson AE *et al.,* 2013)[47]**.**

was proliferating cell nuclear antigen (PCNA); it is a processivity factor that controls the activity of polymerase delta during DNA replication [48]. Fibroblasts retrieved from patients with defective Ligase 1 activity, showed poor lagging strand synthesis [49]. Further studies were done to check whether Ligase 1 is essential for maintaining cell viability. Mice lacking the Ligase 1 enzyme were generated using a gene-targeting method in embryonic stem cells. The

embryos seemed to survive well despite of absence of Ligase 1 clearly suggesting that another ligase is compensating for the loss [50]. Ligation steps of both NER and BER pathways use Ligase 1 for sealing the DNA breaks. Ligase 1 deficiency was identified in a patient with

Figure 3: Structure of human DNA Ligase 1 polypeptide (adapted from Ellenberger T *et al.,* 2008)[44].

missense mutations in different alleles of the *LIG1* gene; typical symptoms of this deficiency included mental retardation, poor growth, immunodeficiency and sensitivity to sunlight. Later, cell lines were developed from the patient and studies showed flaws in DNA replication and repair only [51,52]. VDJ recombination seemed to be functioning normally in fibroblasts extracted from patients with ataxia telangiectasia and Bloom's syndrome, thereby not explaining the reason for causing immunodeficiency [53]. In the similar lines, mice with defective Ligase 1 activity were generated by creating an R771W point mutation, the mice had a poor growth rate along with high genomic

instability in spleen cells, which caused spontaneous epidermal and cutaneous tumours and increased cancer incidence [54].

1.4.2 DNA Ligase 3

The human *LIG3* gene encodes several transcripts. Due to alternative splicing it gives rises to two different transcripts *LIG3*α and *LIG3*β. The *LIG3*α and *LIG3*β further encode two polypeptides each due to alternative translation. Between the two polypeptides, one has a longer sequence as compared to the other (**Fig 4**) [44]. The shorter polypeptide is a nuclear protein. The longer polypeptide comprises of an additional mitochondrial leader sequence (MLS) region at the N terminal[55]. The Ligase 3α polypeptide consists of a BRCT domain where as the Ligase 3β polypeptide has NLS [56] at the C terminal whereas the N terminal consists of a zinc finger and phosphorylated serine residues (Ser123 and Ser210) (**Fig 4**) [57]. They are comprised of a catalytic core where the active lysine site resides [44]. Studies have shown that disruption of the *LIG3* gene in mice resulted in halting embryonic development resulting in embryonic death [58]. Even the expression levels of XRCC1, its interacting partner, were unhindered after the targeted mutation[58,59].

1.4.3 DNA Ligase 4

DNA Ligase 4 is an ATP-dependent ligase, which is encoded by the *LIG4* gene. The first human cDNA clone of the Ligase 4 enzyme was

cloned, sequenced and mapped from human cell nuclei [60]. Studies suggest that the XR-1 cell line, which is deficient in *XRCC4* gene encoding the XRCC4 nuclear phospho protein, is also negative for expression of Ligase 4 protein. However, the introduction of the human XRCC4 cDNA clone into the altered cell line leads to the positive expression of Ligase 4, clearly suggesting that the expression and function of XRCC4 and Ligase 4 enzyme are interdependent [61]. Improper functioning of Ligase 4 due to defects in the enzyme, leads to malfunctioning of NHEJ pathway. This defect was identified in

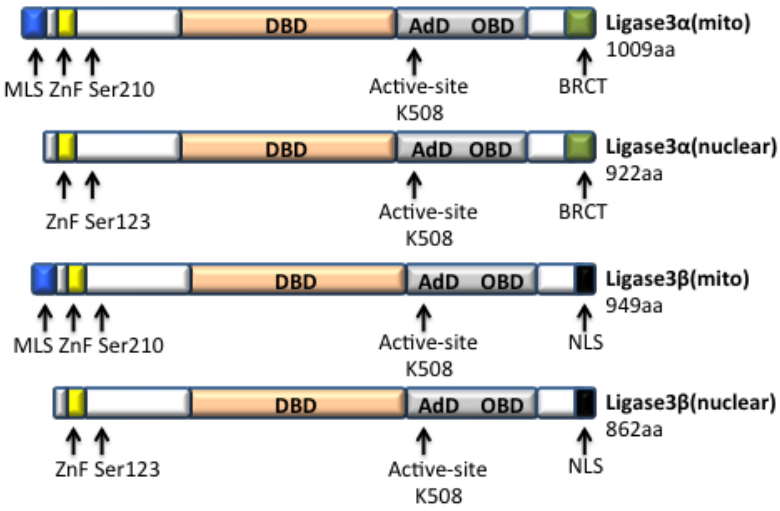

Figure 4 : Structure of human DNA Ligase 3 polypeptides. The Ligase3α (both nuclear and mitochondrial) consist of a BRCT domain where the ligase3β (both nuclear and mitochondrial) consist of an NLS domain(adapted from Ellenberger T *et al.,* 2008) **[44]**.

certain patients who exhibited symptoms such as mental retardation, microcephaly, sensitivity to s, immunodeficiency and genomic

instability [62]. Cell lines derived from these patients were extracted and were studied to identify mutations responsible for causing defects in Ligase 4 activity. A R278H mutation was identified in the Ligase 4 enzyme, which restricts the functioning of the enzyme. A mouse model with this mutation showed signs of retarded growth, sensitivity of irradiation and faulty VDJ recombination [63]. Evidence from research on *LIG4* mutant cell lines clearly implies that cells devoid of *LIG4* gene have low endurance levels upon irradiation making them IR sensitive, similar to that of *XRCC4* mutant cell lines [64]. *LIG4* deficiency is also linked with embryonic death in mice as a result of the lack of lymphocytes due to malfunctioning of VDJ recombination [65]. Unrepaired DNA damage in a cell leads to apoptosis via the p53 pathway; the damage caused is recognized, resulting in the phosphorylated activation of p53. Once p53 is activated it follows any of the two pathways, one where the cell directly undergoes apoptosis and in the other pathway, p53 further recruits and activates downstream transcription factors for apoptosis [66]. The Ligase 4 enzyme requires a high-energy cofactor, like ATP, to catalyse phosphodiester bond formation between the broken DNA strands. The Ligase 4 enzyme, has a multi-domain architecture making it flexible to open and close around DNA. The Ligase 4 polypeptide is made up of 911 amino acids (**Fig 5**). The Ligase 4 polypeptide's catalytic core has

DBD and OBD domains which are active participants in adenylation of the enzyme. The BRCT domains in the C terminal region are responsible for interaction with XLF protein [67]. The N terminus has conserved DBD and catalytic domains.

Figure 5: The domain model of Ligase 4 protein (adapted from Ellenberger T *et al.,* 2008)[44].

The catalytic core further comprises of an adenylation oligobinding domain (AdD) and the active site K213. The C terminus consists of two phospho protein binding BRCT domains, an OBD and a phosphorylated ser650 residue which helps in maintaining the stability of Ligase 4.

1.5 Non Homologous End Joining (NHEJ)

NHEJ is one of the major pathways responsible for repairing DSBs in multicellular eukaryotes, it is the only pathway which assists in making two broken ends of DNA compatible, and helps in fixing them together[68]. NHEJ occurs in the G0/G1 phases of cell cycle [69]. One of the major disadvantages of NHEJ is that it lacks the ability to preserve genomic integrity as during the repair process, a few nucleotides are misplaced at the broken ends [70]. VDJ recombination is a critical step

during B cell differentiation in which the immunoglobulin genes undergo rearrangement to generate the B cell antigen receptor (BCR)[38]. During this process, Recombination activating gene (RAG) proteins cause double stranded DNA breaks that are repaired through the NHEJ pathway.

1.6 Other proteins involved in NHEJ pathway

As well as DNA Ligase 4, there are several key players involved in the NHEJ pathway which play an essential part for successful completion of the repair process; they are Ku 70/80, DNA-dependent protein kinase, catalytic subunit (DNA-PK_{cs}), Artemis, X-ray repair cross complementing protein (XRCC4), XRCC4 like factor (XLF) and DNA Polymerases.

1.6.1 Ku70/80

Ku is a sequence independent DNA binding protein, it is a heterodimer made up of two polypeptides, Ku70 and Ku80, that are abundant in cells [71]. It is one of the first proteins to bind to the broken ends of DNA; it binds to 3' and 5' overhangs and blunt ends produced by irradiation[72]. Its typical toroidal (doughnut) shape allows double stranded DNA to easily slide through it (**Fig 6**), thereby enabling a strong bond with the phosphate backbone of DNA. The translocation of Ku protein along the DNA doesn't require ATP [73]. The two subunits of Ku are made of three domains: an amino-terminal von Willibrand A

domain (vWA), a central core domain and a carboxy-terminal region (CT) (**Fig 7**) . The CT domain of Ku70 consists of an additional SAF-A/B, Acinus and PIAS domain (SAP), while the Ku80 has a longer CT domain to which the DNA-PK$_{cs}$ binds to [74]. Both Ku70 and Ku80 are very similar to each other in structure comprising of the vWA and Ku core domains, the Ku80 polypeptide is slightly longer by 123 amino acids than the Ku70 polypeptide [67].

Figure 6: Typical three dimesional structure reconstruction of a Ku70/80 heterodimer using images from electron microscopy [75].

The three dimensional structure of Ku represents an asymmetric ring, which upon binding to DNA, resembles the bead threading model[71].

Figure 7: Structural representation of Ku heterodimers (adapted from Mahaney BL *et al.,* 2009) [76].

The presence of Ku protein enhances the ligation of incompatible ends via XRCC4-Ligase 4, but the additional presence of XLF along with

XRCC4-Ligase 4 heightens the efficiency of ligation of incompatible ends [77,78].

1.6.2 DNA-PKcs

DNA-PK$_{cs}$ is a polypeptide of 4128 amino acids with a molecular weight of 469 kDa [67]. It is a serine threonine kinase which binds two broken ends of double stranded DNA as these act as a trigger of the kinase activity of DNA-PK$_{cs}$[79]. Ku controls the stimulation of DNA-PK$_{cs}$ depending on the length of DNA, if DNA is longer than 26 bp, Ku activates DNA-PK$_{cs}$ thereby enhancing the stability of binding. A study using the DNA-PK$_{cs}$ assay has confirmed that purified DNA-PK$_{cs}$ kinase activity is stimulated upon binding to double stranded DNA. The kinase activity was entirely dependent on the length of the DNA strand. Specifically, in the presence of long DNA, the kinase activity plummeted in the absence of Ku [80]. DNA-PK$_{cs}$ can phosphorylate another component involved in NHEJ known as Artemis. They form a complex together, resulting in trimming of 3' and 5' overhangs and resolves DNA hairpins due to the strong endonuclease activity of Artemis [81]. DNA-PK$_{cs}$ is activated by auto phosphorylation of the DNA-PK$_{cs}$ activation loop, and this autophosphorylation of protein kinase, on either side of the DNA break, results in proficient end joining [82]. The typical structure of DNA-PK$_{cs}$ comprises of a focal adhesion targeting domain (FAT) at the C-terminus, a Phosphoinositide-kinase domain

(PI3K), a PI3K regulatory domain (PRD), a leucine-rich region (LRR) and a cluster of autophosphorylation sites (**Fig 8**) [67,79]. It has an LRR region between 1502-1539 amino acids at the N terminus of the polypeptide.

Figure 8: The structure of DNA-PK$_{cs}$ (adapted from Mahaney BL *et al.,* 2009)[76].

The region between 3400-3420 amino acids in the FAT domain has a high affinity for Ku binding and the C terminal consists of the auto phosphorylation sites along with the FAT-C domain [67].

1.6.3 Artemis

Artemis is a DNA repair protein encoded by the *artemis* gene, first described in severe combined immunodeficiency (SCID) [83]. The major function of artemis is its 5' endonuclease activity, but when it forms a complex with DNA-PK$_{cs}$, it also acquires 3' endonuclease activity. The Artemis protein is made up of 692 amino acids and consists of a β-lactamase domain, metallo-β-lactamase-associated CPSF Artemis SNM1 PSO2 domain (β-CASP) and eleven DNA-PK$_{cs}$ autophosphorylation sites (**Fig 9**) [84,85]. A H254L mutation in the β-

lactamase domain results in radiosensitivity as observed in SCID[86]. During VDJ recombination, the RAG proteins cause double stranded DNA breaks, thereby generating DNA hairpins at the V, D and J segments[67].

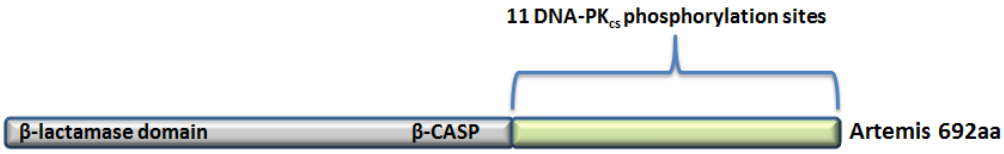

Figure 9: The domain architecture of artemis protein (adapted from Mahaney BL *et al.,* 2009)[76].

The Artemis- DNA-PK$_{cs}$ complex assists in repairing these hairpins. Absence or mutation of Artemis and DNA-PK$_{cs}$ leads to low levels or obstruction of VDJ recombination in humans resulting in lack of B and T lymphocytes [87].

1.6.4 X-ray Repair Cross Complementing Protein (XRCC4)

XRCC4 is one of the main components of the NHEJ Ligase complex that also comprises proteins such as Ligase 4 and XLF. The XR-1 Chinese hamster ovary cell line is defective in DSB repair and VDJ recombination and was critical to identify the *XRCC4* gene[88]. These defective cells were found to be sensitive to IR due to the absence of the *XRCC4* gene. The XRCC4 protein is made up of 334 amino acids (**Fig 10**) [67]. It has an N terminal globular head domain, followed by a long coiled tail at the C terminal. The XRCC4 protein has the ability to

homo-dimerize and tetramarize[89]. It forms a stable complex with Ligase 4 by physical interaction of its long helical coil to the BRCT domains of Ligase 4 enzyme; this interaction stimulates Ligase 4 activity[90,91]. XRCC4 is involved in an adenylation reaction during the DNA ligation step[92].

Figure 10: XRCC4 domain architecture comprising of a head domain made up of 115 amino acids at the N terminus and the coiled coil at C terminus (adapted from Leber R *et al.,* 1998)[93]*.*

XRCC4 is phosphorylated *in vitro* at the C terminal and acts as a substrate of DNA-PK$_{cs}$ thereby linearizing DNA[94]. The ability of the XRCC4-Ligase 4 complex to bind to DNA is promoted by the Ku proteins[95]. The globular head domain of XRCC4 interacts with head domain of XLF to form a complex. Mutations in the XRCC4-Ligase 4 complex cause termination of the NHEJ pathway. Absence of XRCC4 in mice has been associated with improper embryonic development, which eventually leads to their death and also results in neuronal apoptosis[96]. Another study reveals that in the absence of Ligase 4 protein, XRCC4 doesn't migrate to the nucleus upon DNA damage. In this study, the nuclear and cytoplasmic fractions of the normal cells

and *LIG4* deficient cells, were measured for XRCC4 expression. The cytoplasmic fraction of the Ligase 4 deficient cells showed altered XRCC4 expression when compared to normal cells indicating the importance of Ligase 4 protein in nuclear localization of XRCC4 protein[97].

1.6.5 XRCC4 Like Factor (XLF)

XLF was first described in patients with defective DNA repair who were sensitive to IR and had impaired VDJ recombination along with symptoms including growth retardation, microcephaly and immunodeficiency. It has been reported that patients with these symptoms were carrying a mutated XLF gene[98]. Due to the domain similarities between XRCC4 and XLF proteins; the XLF was named after XRCC4 protein as an “XRCC4 like factor”. XLF protein is made up of 299 amino acids; it consists of a head domain and a coiled coil loop region (**Fig 11**).

Figure 11: **Domain architecture of XLF protein** (adapted from Leber R *et al.,* 1998)**[93]**.

Analysis has shown that there are structural similarities between both XRCC4 and XLF proteins, such as they share similar globular head domains and also their long coiled coil domains[93].

Co-immunoprecipitation experiments have confirmed that XLF interacts with XRCC4-Ligase 4 complex both *in vivo* and *in vitro*[93].

1.6.6 DNA Polymerases

DNA polymerases help in synthesising nucleotides and currently, 15 proteins have been described in mammals[99]. DNA DSBs caused by IR, at times cannot be ligated directly by Ligase 4, as they need end trimming and resynthesising of a few nucleotides which is the responsibility of the DNA polymerases[99]. The polλ and polμ polymerases are commonly involved in VDJ recombination [100].

Studies have shown that the polμ co-immunoprecipitates with the Ku heterodimer and also forms a complex with both Ku and XRCC4-Ligase 4 proteins in the presence of DNA[101]. The interaction between the polymerase and the NHEJ factors takes place by the attachment of BRCT domains of polμ to that of Ku70/80 and XRCC4-Ligase 4 complex. Whereas, the polymerases bind to the 5' end of DNA through an 8 kDa domain[99,102]. Mice devoid of polμ were radiosensitive upon being subjected to IR and had stunted DSB repair capacity[103].

1.6.7 NHEJ pathway

The first step of NHEJ involves keeping the broken strands of DNA in

close proximity to each other, a process known as synapsis. Reports suggest that DNA-PK$_{cs}$ might be involved in mediation of synapsis[104]. One of the earliest proteins to be recruited to the broken DNA ends is the Ku heterodimer. It binds to the phosphate backbone of DNA causing a change in the confirmation of the Ku protein[72]. The Ku heterodimer helps in further recruitment of DNA-PK$_{cs}$ and Artemis complex. The DNA-PK$_{cs}$ becomes an active protein kinase upon its contact with DNA and Artemis is responsible for this phosphorylated activation of DNA-PK$_{cs}$[87]. The endonuclease activity of the Artemis-DNA-PK$_{cs}$ complex helps in trimming of the 5' and 3' overhangs thereby generating complementary ends[81]. The DNA polymerases such as polλ and polμ help in filling the gaps, this step is known as end processing[81]. After end processing, the nicks are ligated by the XRCC4-Ligase 4-XLF complex (**Fig 12**)[67].

1.6.8 NHEJ and its role in Cancer

Several findings propose the involvement of the proteins involved in NHEJ in a wide variety of cancers. DNA-PK$_{cs}$ is one of the most widely studied NHEJ proteins. DNA-PK$_{cs}$ activity was measured in the peripheral blood (PB) of untreated cancer patients and also in healthy volunteers.

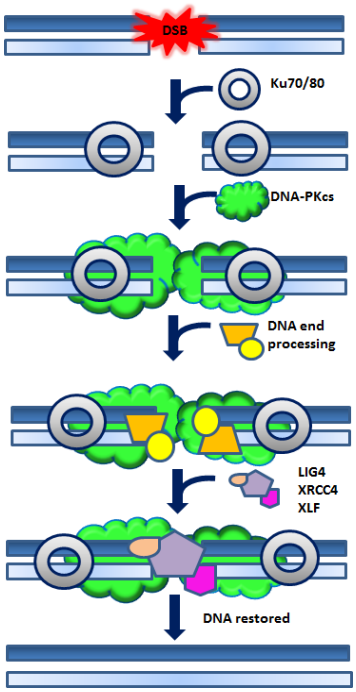

Figure 12: Mechanism of DSB repair by NHEJ pathway (adapted from Lieber MR *et al.,* 2010)[67]***.***

The DNA-PK$_{cs}$ activity in PB from breast and cervical cancer patients was lower when compared to normal individuals. Cytogenetic studies revealed that chromosomal aberrations such as dicentric chromosomes and extra fragments of chromosomes increased with declining DNA-PK$_{cs}$ activity. These outcomes clearly link DNA-PK$_{cs}$ expression and activity to genomic instability and cancer[105]. It has been reported that epidermal growth factor receptor (EGFR) expression increase, or mutation, results in resistance to irradiation. EGFR expression promotes NHEJ by activating DNA-PK$_{cs}$ in malignant glioma and targeting DSB repair pathways might have better

therapeutic outcomes[106]. Studies have shown that increased NHEJ activity in cells to repair DSBs leads to cells becoming resistant to radiotherapy and chemotherapy.The NHEJ pathway is compromised upon continuous exposure to irradiation[107]. Immunohistochemical staining of tumour biopsies taken from cervical cancer patients at different stages, reveal the abundant presence of DNA-PK_{cs} and Ku70/80 positive cells in tumours, which survived radiotherapy confirming the higher expression of these proteins in cervical cancer patients, due to increased NHEJ activity[108]. Increased DNA binding activity of Ku70/80 was observed in tumour biopsies of breast and bladder carcinomas, whereas Ku70/80 repair capacity was reported to decrease in metastatic tumours[109]. Up-regulation of Ku70/80 protein expression and DNA binding activity was detected in tumour samples from human non-melanoma skin cancers[110]. The expression of DNA-PK_{cs} and Ku70 proteins are augmented upon irradiation in oral squamous cell carcinoma[111]. DNA-PK_{cs} and Ku70/80 mRNA and protein levels, were high in tumour tissues of colorectal cancer and this also correlated with high Sp1 expression, suggesting the presence of Sp1 transcription factor in the promoter regions of these proteins[112]. Ku80 (subunit of Ku heterodimer) expression was detected in adult lymphoblastic leukemia and chronic lymphoid malignancies. The Ku80 expression was determined using reverse transcriptase polymerase

reaction where 8.8 and 6.2 mean fold increase in expression was observed when compared to control[113]. The study concludes that having high Ku80 expression will result in poor response to therapy in patients with adult lymphoblastic leukemia[113]. In analyses of genome wide association studies, Ku70/80 and *LIG4* genes have been identified as candidate genes that predispose breast cancer. The study confirms that the presence of variants of Ku70/80 increase the risk of breast cancer, whereas variants of Ligase 4 result in a decreased risk of breast cancer[114]. As mentioned above, DNA-PK_{cs} activity seems to be diminished in most of the cancers, but in lymphoid malignancies, the activity was higher when compared to normal individuals[105]. High grade lymphoma node samples had a greater number of cells positive for DNA-PK_{cs} and Ku protein when compared to low grade lymphoma samples[115]. Patients resistant to treatment with fludarabine and chlorambucil had amplified DNA-PK_{cs} activity[116]. Due to the significant activity of DNA-PK_{cs} in CLL, inhibitors have been designed to target DNA-PK_{cs}. NU7441 is one such inhibitor with IC_{50} value in the range of 0.17- 0.25 µM. Upon treatment with the inhibitor, CLL patients responded better to treatment with drugs such as fludarabine, chlorambucil and mitoxantrone[117]. All of the above evidence clearly suggests the delicate balance of NHEJ in several different cancers. Up regulation or malfunctioning of NHEJ is like a double-edged sword in

terms of cancer. Defects in NHEJ, such as mutations, lead to elevated genotoxic stress in cancer cells whereas hyper-activation results in improved survival of tumour cells[118]. Published studies suggest that downregulation of NHEJ in certain cancers might make the cells more sensitive to chemo-radiotherapy. This can be achieved by seeking inhibitors that target specific proteins involved in NHEJ that can be used as adjuncts for chemotherapy and radiotherapy[118].

1.6.9 Synthetic inhibitors of NHEJ

The core proteins of NHEJ include Ku70/80 complex, DNA-PK$_{cs,}$ Artemis, Ligase 4/XRCC4, Polμ, and Polλ. To date most inhibitors of NHEJ inhibitors target DNA-PK$_{cs.}$ One of the first inhibitors to be generated was Wortamannin, a fungal metabolite, which is a non-specific inhibitor of the PI3K family of which DNA-PK$_{cs}$ is a member [119]. Wortamannin was used to sensitize different mammalian cell lines to radiation and interferes with the joining of DSBs via DNA-PK$_{cs}$[120]. Another PI3K family inhibitor, LY294002, that is structurally different to wortamannin, also effectively radiosensitises cancer cells [121]. NU7026 (2-(morpholin-4-yl) –benzo [h] chomen-4-one), a novel small molecule inhibitor of DNA-PK$_{cs}$ that is more specific in abrogating the activity of the protein, has been tested in leukemic cell lines. Extensive studies have been carried out to investigate the radiosensitization of both quiescent and proliferating cells upon treatment with NU7026 [122]. More

recent studies have focussed on generating inhibitors of downstream proteins in the NHEJ cascade such as Ligase 4[118]. Using crystallography based studies to determine the structure of ligases and drug design technology, compounds which inhibit their binding to DNA have been described. The L89 compound inhibits all the three ligases (Ligase 1, Ligase 3 and Ligase 4) in *in vitro* NHEJ assays[123]. More recently, docking studies were carried out for inhibitors designed to target Ligase 4. This led to the identification of SCR7 as the lead compound for further studies. SCR7 prevents Ligase 4 protein from binding to DNA by competitive inhibition (**Fig 13**). This results in blocking of the NHEJ pathway causing an accumulation of unrepaired DSBs[124]. In mouse models of breast cancer, SCR7 resulted in a decrease of tumours when compared to untreated controls.

In terms of B cell and T cell development, mice treated with SCR7 showed decreased levels of VDJ recombination when compared to their untreated controls, thereby decreasing the lymphocyte count.

To further explore the potential of the SCR7 inhibitor, mice models with Dalton's Lymphoma were irradiated and treated with SCR7 inhibitor. The combination of SCR7 inhibitor and irradiation led to an improved shrinkage in tumour size. Furthermore, when combined with the chemotherapeutic drug etoposide, SCR7 led to a further reduction in tumour growth. Both the above experiments suggest that SCR7

enhances the sensitivity of cancer cells to irradiation and chemotherapy[124].

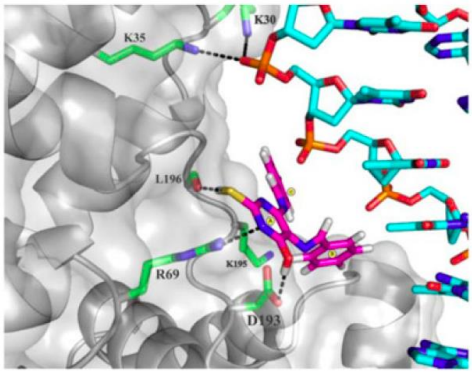

Figure 13: Structure showing interactions between DNA binding domain of Ligase 4 protein and SCR7 inhibitor. The grey cartoon model represents the DNA binding domain of Ligase 4, the coloured sticks represent SCR7 and the black dashes represent the hydrogen bonds between them[124].

1.7 Chronic Lymphocytic Leukaemia

Chronic Lymphocytic Leukaemia (CLL) that is characterised by the amassing of mature B-lymphocytes in blood, bone marrow and lymphoid organs. This accumulation results in leukocytosis, lymphadenopathy, hepatosplenomegaly and bone marrow failure[125]. Most of the patients are asymptomatic, with the disease being diagnosed by increased abnormal white blood cell count. CLL can be distinguished from other B cell disorders due to a distinct surface marker (CD5+ 23+ sIg weak) expression[126]. CLL cases can be categorised based on the rearrangement of immunoglobulin heavy chain genes (IGHV) and can thus be classified as being either mutated

or unmutated[127]. The subsets have different clinical treatment and outcome. Some of the most common genetic lesions observed in CLL are 13q14 (*mir15a* and *mir161*), 11q23 (ataxia telangiectasia-mutated; *ATM*), trisomy 12 and 17p13 (*TP53*)[128]. The most commonly used clinical staging systems are Rai and Binet with risks being classified into low, intermediate and high[129,130]. Some of the prognostic factors which are unfavorable to CLL treatment include advancing age, stage (Rai III and IV or Binet C), shorter doubling time of lymphocytes and increased percentage of prolymphocytes[131]. Coming to treatment of CLL, there is no cure for the disease, however the most commonly used treatments include usage of alkylating agents and purine analogues which inhibit DNA transcription and synthesis. Purine analogues have shown to be better for treatment in terms of response rates and progression free survival on comparison with alkylating agents[131,132]. Fludarabine is one such purine analogue, an inhibitor of DNA polymerase, which is being used extensively for treating CLL. Immunotherapy using Rituximab, a monoclonal antibody against CD20 protein present on the surface of B cells, in combination with chemotherapy is being used as front line treatment known as immunochemotherapy[131,133]. The above mentioned evidence in section 1.6.9 suggests that some of the key components of the NHEJ pathway have a distinct role in different cancers.

1.7.1 DNA damage in CLL

One of the most common features of CLL is the presence of chromosomal abberations. Studies have shown that there are several CLL driver genes with persistent mutations that are involved in cell cycle and DNA repair[134]. Two of the main kinases which help in recognising the DNA damage and alerting the cell for repair are the Ataxia Telangiectasia Mutated gene / Checkpoint Kinase 2(ATM, CHK2) and Ataxia Telangiectasia and Rad 3 related protein/ Checkpoint Kinase 1(ATR, CHK1). The ATM/CHK2 proteins are triggered in order to activate repair pathways for DSBs and ATR/CHK1 proteins are triggered to activate repair pathways for bulky lesions and SSBs[135]. Upon irradiation ATM gets phosphorylated at the Serine-1981 residue and as a result, ATR is recruited by RPA-bound single stranded DNA complex[135]. The active ATM helps in phosphorylation of its downstream substrate CHK2 at Threonine-68[136]. CHK1 is activated by the ATR-mediated phosphorylation of its two Serine residues 317 and 345[137]. Both these kinases - ATM/CHK2 and ATR/CHK1 – eventually activate the Cyclin dependent Kinase 25 (Cdc25) and promote division of cells[138]. If successful DNA repair cannot be achieved, these pathways trigger the apoptotic cascade mediated in a p53-dependent manner [139]. The ATM gene in CLL is mutated in 36% of cases resulting in patients responding poorly to chemotherapy due

to weakened DNA DSB repair[140]. The p53 mutations result in poor prognosis in CLL patients and more than 76% of them are missense mutations[128]. In CLL, the ATM-CHK2-p53 pathway plays a major role in triggering the programmed cell death, but mutations of p53 and ATM genes result in poor response of patients to conventional chemotherapy[134]. The ATM is largely involved in stimulation and increase of p53 expression thereby activating its transcriptional activity and triggering its downstream targets that are involved in apoptosis and cell cycle arrest[141]. CLL cases with 17p deletion are known to be resistant to standard chemotherapy but upon treatment with BCR pathway inhibitors such as the inhibitors of Bruton Tyrosine Kinase (BTK), these cases demonstrated significant improvement[142]. CLL patients treated with combination of Idelalisib, a PI3K inhibitor along with Rituximab responded better in terms of reduced lymphadenopathy irrespective of the high risk prognostic factors[143]. In similar lines, we set out to explore if the DNA Ligase 4 inhibitor (SCR7) has a potential therapeutic role in CLL. In order to do so, we inititiated this study to determine the expression of DNA ligases in primary CLL samples.

Aims

The aims of my project were:

1) **To investigate the expression of DNA Ligases in CLL:**
    a) Examine the mRNA expression levels of *LIG4*, *LIG3* and *LIG1* in both B- cell lines and primary CLL samples.
    b) Determine the protein expression of Ligase 4 in a cohort of CLL cases.
2) **Observing whether the expression levels in CLL cells are affected by irradiation.**
3) **Examining the effects of a novel Ligase 4 inhibitor, SCR7, on cell behaviour.**
    a) Investigating if SCR7 affects cell viability both alone and in combination with irradiation and/or DNA damaging agents.

Chapter 2: Methods

2.1 Cell culture

2.1.1 Cell line culture and maintenance

Cells were cultured under sterile conditions. Complete Dulbecco's Modified Eagles medium (DMEM) (Sigma Aldrich, UK) was made by adding Fetal Calf Serum (FCS) (10 %, BioSera, UK), L-glutamine (2 mM, Sigma Life sciences, UK) and Penicillin-Streptomycin (1000 units, 1 mg, Sigma Life Sciences, UK). Complete Roswell Park Memorial Institute medium (RPMI-1640) (Sigma Life Sciences, UK) was made by adding 10 % Fetal Calf Serum and Penicillin-Streptomycin (as above).

2.1.2 Cell thawing

One vial of frozen cells from a -140 °C freezer was retrieved and was thawed in a water bath at 37 °C. The vial was quickly wiped with ethanol before transferring it to the laminar air flow hood. The cells were washed in the media by spinning them down for 5 minutes at 500 rcf. The supernatant media containing Dimethylsulphoxide (DMSO, Sigma Aldrich, UK) was discarded and the cells were re-suspended in 5 mL complete media and transferred into a T-25 cm^2 culture flask and were grown in an incubator set at 5 % CO_2 at 37 °C (humidified).

2.1.3 Cell line passaging

Suspension cells: For sub-culturing of suspension cells, the cells were counted manually using a haemocytometer and trypan blue dye (Sigma Aldrich, UK) and the viability was measured. The required numbers of cells were transferred into a new culture flask and the volume topped up with fresh complete media and the flask was placed in a 5 % CO_2 incubator at 37 °C (humidified).

Adherent cells: Sub-culturing of adherent cells was performed once the cells were confluent enough in the flask by observing under a microscope. The media were removed and the cells were washed with phosphate buffered saline (PBS). Then the monolayer of cells was trypsinised using trypsin- ethylenediaminetetraacetic acid (EDTA) (Sigma Life Sciences, UK) for 2 to 5 minutes. The trypsin was neutralised by adding fresh complete media to cells. Then the cells were counted using a haemocytometer by staining them with Trypan blue dye to check cell viability and the required numbers of cells were transferred to a fresh flask. Complete media was then added and the flask was placed in a 5 % CO_2 incubator at 37 °C (humidified).

2.1.4 Cell line freezing

Freezing media comprising of 10 % DMSO in complete media was prepared. The cell viability and count was determined manually using a haemocytometer and trypan blue. The cells were centrifuged at

500 rcf for 5 minutes and the supernatant was removed carefully. The cells were resuspended in the required volume of freezing media to give 1 mL of cells at $1x10^7$ viable cells. This was aliquoted into each cryovial and frozen at -80 °C overnight and then transferred to -140 °C freezer for storage.

Cell line	Culture Method	Media used
HeLa	Adherent	DMEM
K562	Suspension	RPMI
MEC1	Suspension	DMEM
Daudi	Suspension	RPMI

Table 1: List of cell lines used and culture method.

2.2 Molecular Biology

2.2.1 RNA extraction

An RNeasy kit (Qiagen, UK) was used to extract RNA from cells and the given protocol was followed accordingly. A cell pellet containing a maximum of $1x10^7$ cells was thawed on ice and to it, 600 µL of RLT buffer with 10 µL of β mercaptoethanol (National Diagnostics, UK) was transferred into a QIAshredder placed in a collection tube. The lysate was centrifuged for 2 minutes at 10000 x g. To the supernatant one volume of 70 % ethanol was added and mixed well by pipetting and

applied to an RNeasy mini spin column placed in a 2 mL collection tube (700 µL) which was centrifuged at 8000 x g for 15 seconds. The flow through was discarded and the step repeated for the remaining volume. For DNase digestion, 350 µL of RW1 buffer was added to the RNeasy spin column and was centrifuged for 15 seconds at 8000 x g. The flow through was discarded in all of the above steps. To 70 µL RDD buffer, 10 µL of the DNase I stock solution was added to prepare DNase I incubation mix. The contents were mixed gently by inverting the tube. In the next step, 80 µL of the DNase I incubation mix was added to the RNeasy spin column membrane and was incubated at room temperature for 15 minutes. The column was washed with 350 µL of RW1 buffer by centrifuging for 15 seconds at 8000 x g. Later, 500 µL of RPE buffer was added to the RNeasy spin column and was centrifuged for 15 seconds at 8000 x g. Again, 500 µL of RPE buffer was added to the RNeasy spin column and was centrifuged for 2 minutes at 8000 x g. The flow through was discarded in the above steps. The RNeasy spin column was placed in an empty tube and was centrifuged at full speed for one minute in order to dry the membrane. The RNA was eluted by placing the RNeasy spin column in a new 1.5 mL collection tube. In the column, 30 µL of nuclease free water (NFW) was added and centrifuged for 1 minute at 8000 x g. The

concentration of RNA was measured using a NanoDrop machine (Thermo Scientific NanoDrop 2000, USA).

2.2.2 cDNA synthesis protocol

For generating cDNA in a single reaction in the first step, 1 µg of RNA was taken, to which 1 µL of Oligo(dT)$_{12-18}$ Primer (Life Technologies, UK), 1 µL 10 mM dNTP Mix (Life Technologies, UK) were added along with NFW to make up to a final volume of 12 µL in an RNase free tube. All volumes that are described are for one reaction. The contents of the tube were mixed well by pipetting and were placed on a heat block at 65 °C for 5 minutes. Next, 2 µL of 0.1 M Dithiothreitol (DTT) (Life Technologies, UK) and 4 µL of 5x First-Strand Buffer (Life Technologies, UK) were added to the tubes and were mixed thoroughly and heated at 42 °C for 2 minutes. Lastly 1 µL of SuperScript II Reverse Transcriptase enzyme (Life Technologies, UK) was added to the reaction and the tubes were heated at 42 °C for 50 minutes and then at 72 °C for 15 minutes. To prepare a negative control, 1 µL of NFW was used in place of 1 µL SuperScript II Reverse Transcriptase enzyme. The cDNA synthesised was stored at -20 °C.

2.2.3 Polymerase chain reaction (PCR)

For a single 25 µL reaction in a 0.5 µL PCR tube, 22 µL of Platinum® PCR SuperMix High Fidelity (Life Technologies, UK), 1 µL of forward primer and 1 µL of reverse primer (stock concentration 100 µM,

working concentration 2.5 µM, final concentration 0.1 µM) were mixed . For multiple reactions, a master mix was made. To the relevant tubes, 1 µL of cDNA template was added. A negative control was set up using the above reagents and 1 µL of NFW, in place of the cDNA template. All the tubes were centrifuged briefly and placed in the thermo cycler. The following thermal profile was used:

95 °C 10 minutes (x1)

95 °C 20 sec, annealing temperature15 sec, 72 °C 30 sec (x34)

72 °C 10 minutes (x1)

Hold at 4 °C

2.2.4 Agarose gel electrophoresis

The amplified PCR product was analysed by running it on an agarose gel containing ethidium bromide (EtBr, Promega, UK). Agarose (Web Scientific, UK) was measured using a weighing balance and 2 g was added to 100 mL of 1X Tris-Borate-EDTA buffer (TBE), (Sigma Aldrich, UK) and heated in a microwave until the agarose was dissolved completely. The melted agarose solution was allowed to cool at room temperature after which 8 µL of EtBr was added to it and mixed slowly. The solution was poured into a gel casting tray, pre-fixed with a comb, and the contents were allowed to solidify. The gel was transferred into an electrophoresis tank containing 1X TBE buffer. To the PCR products, 6X loading buffer (10 mM Tris-HCl, pH 8.0), (Fisher

Scientific, UK), 50 mM EDTA, 15 % Ficoll-400, 0.5 % Orange G, (Sigma Aldrich, UK) was added and then loaded onto the gel along with a DNA ladder. The electrophoresis chamber was closed and the gel was run at 100 V for 45 minutes. After running, the gel was visualised was to verify the PCR products using a UV trans illuminator (UVITEC, UK).

2.3 Protein analysis

2.3.1 Cell lysis and protein determination

Whole cell lysates were prepared from $1x10^7$ viable cells. Cells were counted manually using a haemocytometer and Trypan Blue dye. The required number of cells were pelleted at 500 x g and washed with ice cold PBS. The supernatant was aspirated completely. To the pellet of cells, 200 µL of clear lysis buffer (1 % SDS, 50 mM Tris, pH 6.8, 5 mM EDTA and 10 % Glycerol, (Fisher Scientific, UK)) was added along with 2 µL of complete protease inhibitor cocktail (Calbiochem, UK) and incubated on ice for 30 minutes. The whole cell lysate was sonicated on ice and clarified for 10 minutes, maximum speed of 10000 x g, at 4 °C. The supernatant was transferred to fresh tubes and stored at -20 °C until ready for use. The protein concentration of the lysates was measured using the Bio-Rad *DC* Protein Assay kit. A sufficient volume of Reagent A was prepared using 20 µL of Reagent S added to 1 mL of Reagent A. Protein standards from 0.5 mg/mL to 3 mg/mL protein

were prepared using bovine serum albumin (BSA) prepared in the same lysis buffer as the sample. To a 96 well plate, 5 µL of standard or sample were pipetted. To each of the wells, 25 µL of the Reagent A' was added, followed by pipetting of 200 µL of Reagent B into each well. The plate was gently agitated to mix the reagents and incubated at room temperature. After 15 minutes, the absorbance of the samples was read at 750 nm using an FLx800 fluorescence microplate reader (BioTeK, USA).

2.3.2 Western blotting

To analyse protein expression, 10 % resolving and 4 % stacking gels were prepared. The resolving gel was made using 7.05 mL distilled water, 4.25 mL of resolving buffer (Geneflow, UK), 5.7 mL of acrylamide (Sigma Aldrich, UK), 50 µL of 10 % ammonium per sulphate (APS) and 15 µL of N, N, N', N' Tetramethylethylenediamine (TEMED, Sigma-Aldrich, UK). After the resolving gel was solidified, stacking gel was made using 4.6 mL distilled water, 1.9 mL stacking buffer (Geneflow, UK), 1 mL of acrylamide, 50 µL of 10 % APS and 15 µL of TEMED. Ten micrograms of whole cell lysate was diluted in 4x sample loading buffer (8 % SDS, 40 % glycerol, 20 % β-mercaptoethanol, 0.008 % bromophenol blue (Sigma Aldrich, UK) and 250 mM Tris (pH 6.8)) and boiled at 95 °C for 5 minutes. The prepared samples were loaded onto the gel along with a suitable molecular

weight marker. The gel was run at 30 mA for 60 minutes in an electrophoresis chamber filled with 1X running buffer (25 mM Tris, 190 mM glycine (Fisher scientific, UK), and 0.1 % SDS). The proteins were transferred from the polyacrylamide gel to a Polyvinylidene fluoride (PVDF) membrane (Roche, UK) using a wet transfer system. The membrane was pre-soaked in methanol and was sandwiched between sponges pre-soaked in 1X transfer buffer (25 mM Tris, 190 mM glycine), and filter paper. The enclosed sandwich was placed in the tank containing 1X transfer buffer. The transfer was performed at 75 V for 60 minutes. After transfer, the membrane was blocked using non-fat milk powder (3 %) dissolved in 1X TBS-Tween 20 (0.05%) solution for 60 minutes at room temperature with agitation. Following blocking, the membrane was incubated with the chosen primary antibody (**Table 2**), diluted to the required concentration, in blocking solution. The membrane was incubated with the antibody overnight at 4 °C with agitation. Following incubation, the membrane was washed thrice at 5 minute intervals with 1X PBS-Tween 20 (0.05 %) solution. After the washes, the membrane was incubated with desired secondary antibody diluted 1:5000 with blocking solution at room temperature for 60 minutes, with agitation. After incubation, the membrane was washed as described above. The protein bands were detected using ECL (Immobilon western chemiluminiscent HRP substrate Millipore,

USA) or ECL advanced kits (Westar Supernova, Gene flow, UK) and digital images were captured using a luminescent image analyzer (FUJIFIL LAS1000, Japan).

Antibody	Dilution
Ligase IV antibody (Abcam, UK)	1:1600
XRCC4 antibody (AbD Serotec, UK)	1:2000
P53 antibody (Oncogene Research group, USA)	1:1000
Goat-anti-mouse-conjugated secondary antibody Santa cruzBiotechnology, USA)	1:5000
Goat-anti-rabbit HRP-conjugated secondary antibody (Santa cruz Biotechnology, USA)	1:5000
Mouse Monoclonal Beta actin antibody (Sigma-Aldrich, UK)	1:10000

Table 2: The above table comprises of the list of antibodies and their respective final dilutions used for studying protein expression.

2.4 Measurement of cell proliferation using a colorimetric BrdU ELISA assay

The assay is based on the incorporation of the pyrimidine analogue 5-Bromo-2'-deoxyuridine (BrdU) into the genomic DNA of replicating cells. Different cell lines (Daudi, HeLa and MEC1) were cultured and treated with varied concentrations of SCR7 inhibitor (Kind gift from Dr. Sathees Raghavan) (10 µM, 50 µM, 100 µM, 250 µM) alone and in combination with irradiation (5 Gy). Approximately 1 x 10^4 cells were

seeded in each well of a 96 well plate in triplicate according to their treatments, in a final volume of 100 µL. To each of the wells 10 µL of BrdU (10 µM stock concentration, final concentration 1 µM) labelling solution was added (now labelling medium) and incubated at 37 °C for 2 hours before the completion of time points. The labelling medium was removed carefully (plates containing suspension cells were first centrifuged at 300 x g for 10 minutes) using a pipette. Once the labelling media was removed, the cells were subjected to drying at 60 °C for 1 hour. After the cells were dried, 200 µL FixDenat solution (Roche, UK) was added to each of the wells and the plates incubated for 30 minutes at room temperature. The FixDenat solution was removed by flicking the plate and tapping on absorbent paper. For one 96-well plate, dilute 100µL Anti-BrdU-POD stock solution in 10 mL antibody dilution solution. One hundred microlitres of anti-BrdU-POD working solution was added to each of the wells and the plate incubated for 90 minutes at room temperature. The anti-BrdU-POD working solution was removed by flicking the plate and the wells washed three times using 200 µL of washing solution (Roche, UK). The washing solution was removed by flicking the plate and 100 µL substrate solution (Roche, UK) added to each of the wells. The solution was left in the well until a colour change was observed across the wells (approximately 5-30 minutes). Once the colour development

was sufficient for measurement, the reaction was stopped by the addition of 25 µL 1 M sulphuric acid to each well. The plate was placed on a shaker for 1 minute in order to mix the contents thoroughly and the absorbance was measured within 5 minutes using an ELISA reader (FLX800 microplate reader; BioTeK, USA) at 450 nm.

2.5 Measuring apoptosis of cells by flow cytometry using PI and DiOC6

Daudi, MEC1 and HeLa cells were used to perform apoptosis assays. One hundred microlitres of cell suspension ($1x10^4$ viable cells) was taken into a polypropylene tube (Beckman Coulter, Epics XL MCL, UK). Propidium Iodide (PI) (100 mg/mL; Sigma, UK) and 3,3'-dihexyloxacarbocyanine iodide (DiOC6) (60 mM; Molecular Probes, UK) were diluted in PBS to concentrations of 2 mg/mL and 40 mM respectively. To each of the cell samples, the diluted DiOC6 was added such that the final concentration was 40 nM and the samples were incubated in the dark at 37 °C for 20 minutes. Following this, the diluted PI solution was added to the samples such that the final concentration was 1 µg/mL. The sample and dye were mixed gently and were placed in the incubator at 37 °C, 5 % CO_2 for 5 minutes. The samples were then analysed by flow cytometery (FACScalibur, Beckman Coulter, UK).

2.5.1 Measuring apoptosis of cells upon treatment with irradiation only

HeLa and MEC1 cells were seeded in 24 well plates at a density of 5 x 10^4 cells/well. The following morning, cells were treated with irradiation (3 Gy or 5 Gy) and returned to the 5 % CO_2 incubator at 37 °C. Apoptosis was measured, following the method described in section 2.5 after 24, 48 and 72 hours.

2.5.2 Measuring cytotoxicity and radiosensitivity of cells upon treatment with different concentrations of SCR7 inhibitor and irradiation

For the cytotoxicity and radiosensitivity experiments, Daudi and MEC1 cells were seeded in 24 well plates at a density of 5 x 10^4 cells/well. The SCR7 inhibitor was diluted with DMSO therefore, negative controls where prepared for both experiments with 0.1% DMSO and untreated cell lines also included. To determine the cytotoxicity, after the cells were seeded the previous day, they were treated with 5 Gy irradiation by placing the cells in a tube and they were replaced into the plate, and then incubated in the presence of the SCR7 inhibitor at 10 µM, 50 µM, 100 µM, and 250 µM. As the inhibitor was dissolved in DMSO, a negative control consisting of 0.1% DMSO only was also included. An untreated sample of each cell line was also included. The cells were harvested at 24 hours and 48 hours and apoptosis was measured by following the method in section 2.5. To determine the

radiosensitivity following the seeding of Daudi and MEC1 cells the previous day in 24 well plates at a density of 5 x 10^4 cells/well they were treated with varied concentrations of SCR7 inhibitor (10 µM, 50 µM, 100 µM, and 250 µM). After 24 hours the cells were exposed to 5 Gy irradiation and were replaced in the 5% CO_2 incubator at 37 °C. The SCR7 inhibitor was diluted using DMSO. Negative controls consisting of 0.1% DMSO only and untreated samples without inhibitor and irradiation were also included. For both the experiments, the cells were harvested at 24 and 48 hours following irradiation treatment to study cell death by following the method in section 2.5.

2.6 Statistical analysis

The data was analysed to measure statistical significance using Two way ANOVA for data generated for MEC1 cells by cytotoxicity assay and Daudi cells by BrdU assay. Prism 5 software and microsoft excel were used to carry out these tests.

Chapter 3: Results

3.1 Verifying cDNA quality using *GAPDH* primers

The cDNA synthesised from a variety of cell lines (MEC1, PC3, 22RV1, H417, K562, HUT78, HeLa and Daudi) was verified for quality by PCR using *GAPDH* primers (**Table 3**). PCR products were analysed by agarose gel electrophoresis as described in Chapter 2 and results shown in (**Figs 14 a and b).**

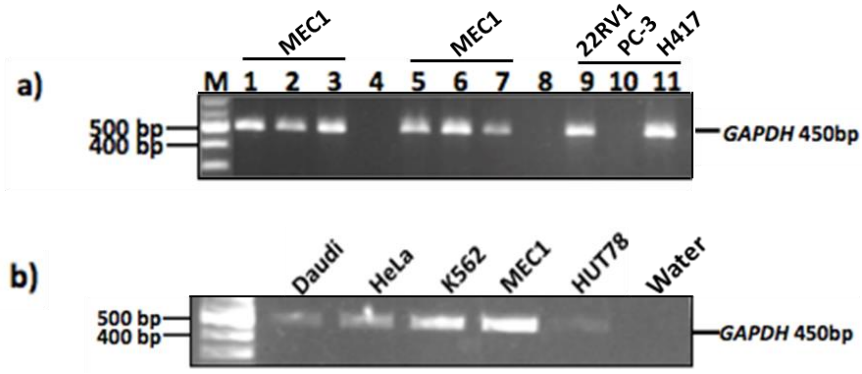

Figure 14: Verifying cDNA quality using *GAPDH* primers
PCR amplification of cDNA (from MEC1, 22RV1, PC3 and H417 cell lines) using *GAPDH* primers was performed and the reactions were analysed by agarose gel electrophoresis.**(a)** Lanes 1, 2 and 3 show the amplification of MEC1 cDNA from a single aliquot. Lanes 5, 6 and 7 are amplifications of 3 independent MEC1 cDNA samples. Lanes 9, 10 and 11 are amplified products of cDNAs prepared from 22RV1, PC3 and H417 cells. Lane M: 100 bp DNA ladder (New England Biosciences, UK). **(b)** PCR amplification of GAPDH primers using cDNA from Daudi, HeLa, K562, MEC1 and HUT78 cDNA's.

Successful amplification, indicated by the presence of a single band at 450 bp, was detected from amplifications of all independent aliquots of

MEC1 22RV1, H417, K562, Daudi, HeLa, HUT78 and K562 cDNAs (**Figs 14 a-b**), but not PC3 cDNA (**Fig 14a**, lane 10) which was likely due to failure of cDNA synthesis. Having confirmed the cDNA quality obtained from MEC1, 22RV1, H417, K562, Daudi, HeLa, HUT78, these were used for further experiments.

3.2 Optimisation of annealing temperature of primers specific for DNA ligases

Several different primer sets were designed (**Table 3**) to examine the expression of *LIG1*, *LIG3* and *LIG4* mRNA. Gradient PCRs were performed where the PCR reaction mixtures were subjected to a range of temperatures (52 °C to 65 °C) to ascertain the optimal annealing of the primer sets. K562 and MEC1 cDNA were used as templates for analysis. Representative gel images are shown below in (**Fig 15a, b, c and d)**. Two independent sets of primers for the *LIG1* gene were designed to generate amplicons of 148 bp and 110 bp respectively. Though amplification was observed at 52 °C, 53.7 °C and 56.3 °C for both the primer sets, several non-specific bands (representative non-specific bands are highlighted in red) were detected above the appropriate amplicon (**Fig 15a and b**). At 58 °C non-specific bands are seen along with required amplification (**Fig 15b**) for both sets of *LIG1* primers and at higher temperatures such as 60.5 °C and 62 °C, the intensity of amplification decreased (**Fig 15b and c**).

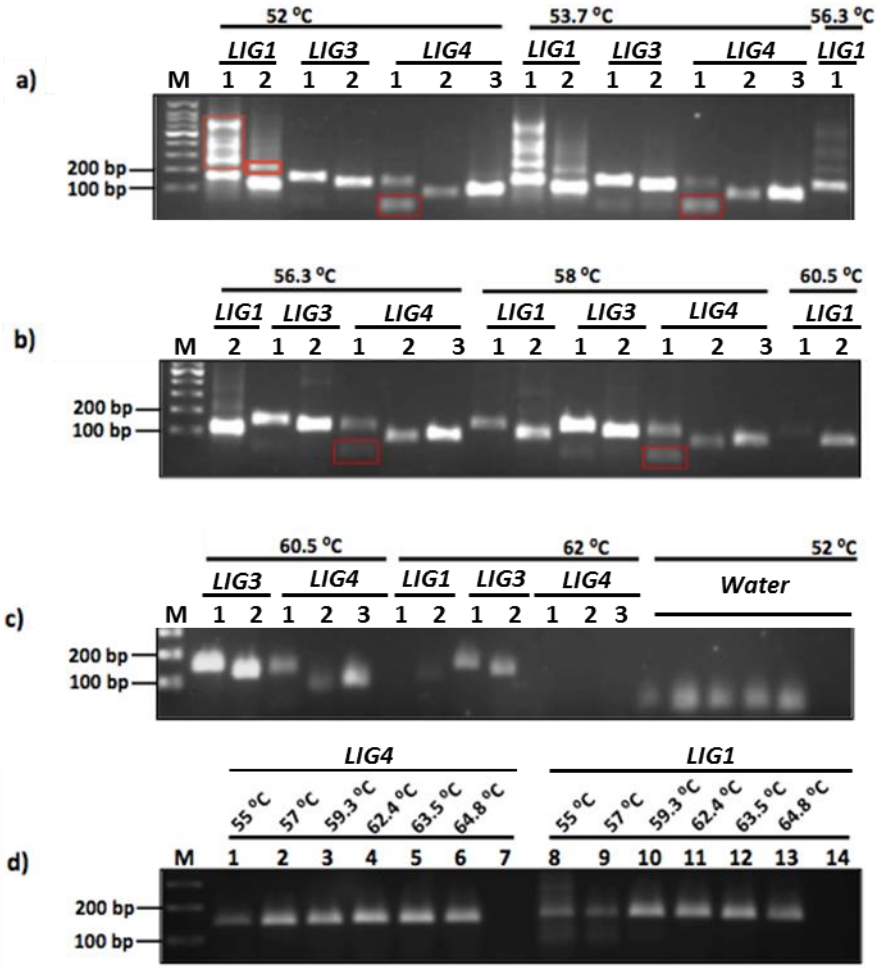

Figure 15: Gradient PCR of primer sets to determine optimal annealing temperature(a, b & c). Gradient PCR was performed to determine the optimal annealing temperatures of *LIG1* primer (sets 1 and 2), *LIG 3* primer (sets 1 and 2) and *LIG4* primers (sets 1, 2 and 3). K562 cDNA was used as the template. The temperature ranges from 52 °C to 62 °C are shown.The sizes of amplicons for *LIG1* sets 1 and 2 are 148bp and 110bp, *LIG3* sets 1 and 2 are 150bp and 136bp and lastly for the three sets of *LIG4* are 136bp,90bp and 100bp. The negative controls of the PCR reaction for all the primer sets were run at 52 °C with water. Highlighted red boxes indicate non-specific bands. **(d)** Gradient PCR using *LIG4* set 4 primer set and *LIG1* primer set 1, with MEC1 cDNA and K562 cDNA as templates, were performed to identify ideal annealing temperatures.The expected amplicon sizes for *LIG4* set 4 in lanes 1 to 6 are 154bp and *LIG1* set1 primers in lanes 8 to 13 are 148 bp respectively. Lanes 7 and 14 are the negative controls for the PCR reaction. The primer sets have been mentioned in detail in Table 3.

Similarly for the both the *LIG3* primer sets the appropriate amplicons were detected at 150 bp and 136 bp respectively (**Fig 15a and b**). The bands were detected consistently throughout the temperature gradient, but high intensity amplified bands were detected at 58 °C suggesting that this was the ideal annealing temperature (**Fig 15b**). Lastly, the three sets of *LIG4* primers were designed to generate 136 bp, 90 bp and 100 bp amplicons. *LIG4* set 1 primers showed a non-specific band (**Fig 15a and b**) and *LIG4* set 2 primer set displayed faint amplification consistently across the whole temperature gradient (**Fig 15a and b**). Only *LIG4* primer set 3 generated a single strong band throughout the temperature gradient (**Fig 15a and b**). Due to contamination problems with PCR, an additional primer set was designed for *LIG4* gene, which amplified a 154 bp region of the cDNA. The intensity of amplification was consistent along the temperature gradient from 55 °C to 64.8 °C (**Fig 15d**) in lanes (1 to 6).

Gene	Primer order	Sequence	Length	Tm (°C)	Amplicon size
LIG1 set 1	FP	5'gacagagaagccaagaggaag3'	21	54	148bp
	RP	5'ctgctttggaggtctttaggg3'	21	54	
LIG1 set 2	FP	5'gtgtgggaggtgaagtgc3'	18	53	110bp
	RP	5'cgaataaaccgagggaagcg3'	20	54	
LIG3 set 1	FP	5'gaggcagctatatgtctttggc3'	22	55	150bp
	RP	5'cagatctgcttcatggacatcc3'	22	55	
LIG3 set 2	FP	5'cagccaagcccaacaactctg3'	21	56	136bp
	RP	5'cgccatggtggccgataatc3'	20	56	
LIG4 set 1	FP	5'gctgggattctctggttcac3'	20	54	136bp
	RP	5'cacaaatctgcaaaaggaacgtg3'	23	53	
LIG4 set 2	FP	5'tctgcaagccgcagttaaa3'	19	49	86bp
	RP	5'ggaacgtgagatgcaacag3'	19	51	
LIG4 set 3	FP	5'atggagatgctggagactttg3'	21	52	100bp
	RP	5'aggtcgtttacttgctgtatgg3'	22	53	
LIG4 set 4	FP	5'cctggaactgtattgcctgc3'	20	58.9	154bp
	RP	5'gcccgaggccagttaaacgag3'	21	58	
GAPDH	FP	5'agccacatcgctcagaacac3'	20	60	450bp
	RP	5'gaggcattgctgatgatcttg3'	21	60	

Table 3: Characteristics of primers used for PCR amplification of *LIG1*, *3* and *4* genes along with *GAPDH* primers as seen in Figures 14 and 15.

Gene	Primer order	Sequence	Length	Tm (°C)	Amplicon size
LIG1 set 3	FP	5'gtgtgggaggtgaagtgc3'	18	53	148bp
	RP	5'cgaataaaccgagggaagcg3'	20	54	
LIG3 set 3	FP	5'gagaaggaacagataacccagc3'	22	55	148bp
	RP	5'tggtactggtgacaaatgaggc3'	22	55	
LIG4 set 4	FP	5'cctggaactgtattgcctgc3'	20	58.9	154bp
	RP	5'gcccgaggccagttaaacgag3'	21	58	

Table 4 : The list of primers used in the next set of experiments(Figure 16 and 17).

3.3 Determination of the expression of *LIG4, LIG3* and *LIG1* mRNA in CLL samples and the human bone marrow stromal cell line (HS-5)

Each of the chosen primer sets were used to amplify specific DNA ligases from cDNA synthesised from primary CLL patient samples and additionally from the HS-5 cell line. Upon PCR amplification using the *LIG4* primer set 4, specific product was observed in all the cases (**Fig 16**). Amplification from the HS-5 cell line cDNA was less robust.

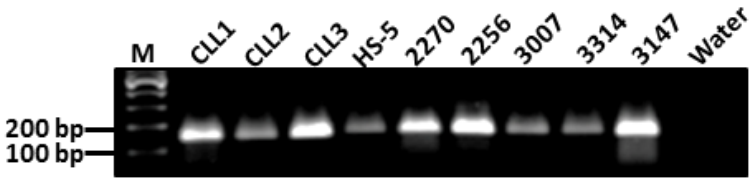

Figure 16: End point PCR using *LIG4* primer set 4 and cDNA extracted from primary CLL patient samples. The expected 154 bp amplified product is seen in all CLL cases the negative control with water was clear.

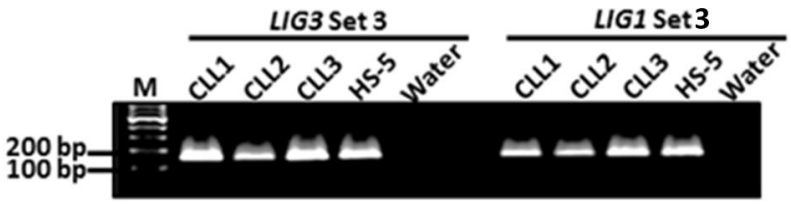

Figure 17: Endpoint PCR of *LIG3* and *LIG1* using described primer sets with cDNA extracted from CLL patient samples. The expected amplicon sizes for both primer sets (*LIG3* set 3 and *LIG1* set 3) are 148 bp. Three different CLL cases along with HS-5 cell line cDNA were used in the PCR reaction.

Further PCR amplification was carried out using *LIG3* and *LIG1* primer sets and cDNA generated from 3 CLL patient samples and HS-5 cell

line. Robust amplification was observed in all the cDNA samples including HS-5 cell line for both the primer sets as seen in (**Fig 17**).

3.4 Analysis of DNA Ligase 4 protein expression in haematopoietic cell lines

In order to establish the conditions, examine the specificity of a commercial antibody to detect Ligase 4 (Polyclonal Antibody, Protein tech, UK) and determine the protein expression whole cell lysates were prepared from cell lines a panel of in house cell lines (Daudi, HeLa, K562, MEC1, HUT78, RHUT78 and RMEC1) from protein analysis as described in the methods section. Two different protein concentrations were used (10 and 20 µg).

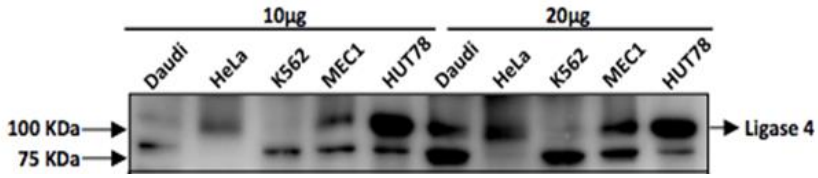

Figure 18: Western blot depicting Ligase 4 protein expression in a panel of lymphoid cell lines using a commercial polyclonal antibody. Whole cell lysates of Daudi, HeLa, K562, MEC1 and HUT78 cells were prepared and 10 µg and 20 µg of protein was loaded onto polyacrylamide gels. After transfer, the PVDF membrane was probed with a Ligase 4 polyclonal antibody (Protein tech, UK; 1:500 dilution). HeLa lysate served as positive control. The expected protein size is 100-104 kDa. The bands appearing around 75 kDa could be non-specific. Equal amount of protein was loaded on to the gel as determined by Bio-Rad *DC* Protein Assay kit.

HeLa cell lysate served as the positive control and Ligase 4 protein expression was readily detected (**Fig 18**). The appearance of a second band at 75 kDa in the Ligase 4 blots prompted us to validate this further. Therefore, an alternate antibody (Anti-DNA Ligase IV

antibody, Abcam, UK) was obtained. The latter antibody did detect a single and strong band in HeLa cell lysates but only faint bands in K562, MEC1 and RMEC1 cell lines (**Fig 19)**.

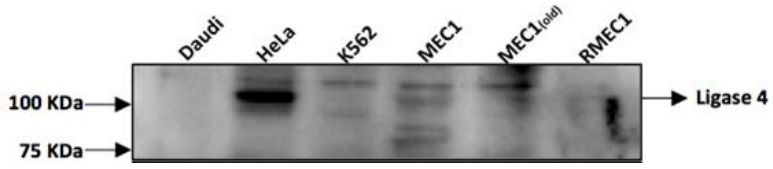

Figure 19: Western blot analysis of DNA Ligase 4 protein expression in cell lines using an Anti-DNA Ligase IV antibody (Abcam, UK). 10 µg of whole cell protein lysates from Daudi, HeLa, K562, MEC1 and RMEC1 were loaded onto a gel and the proteins transferred onto a PVDF membrane and probed with Ligase 4 antibody (1:1600). The expected protein size 109 kDa. A frozen lysate of MEC1 cell line was also used (MEC1old). Equal amount of protein was loaded on to the gel as determined by Bio-Rad *DC* Protein Assay kit.

In parallel, additional experiments were sought to investigate protein expression of DNA Ligase 4 in MEC1 and HUT78 cell lines along with their counterparts that are resistant to Romidepsin, a histone deacetylase inhibitor (HDACI). Romidepsin is licensed for the treatment of cutaneous T cell lymphoma[144]. Previous studies have identified HDACIs as potential DNA damaging agents and suggested that treatment of cells with HDACIs resulted in activation of NHEJ and HR[145]. HDACIs have been reported to increase NHEJ frequency due to generation of DSBs. However, upon prolonged exposure, several human cell lines have been reported to acquire resistance to these inhibitors, most likley due to HR [145]. As XRCC4 is another downstream NHEJ protein which is a key partner of DNA ligase 4 in the DNA

ligation reaction, it's expression was also investigated in these resistant cell lines. Although Ligase 4 protein clearly expressed in HeLa cell lysates, parental MEC1 and HUT78 cells showed only weak expression. There was a hint of upregulation of DNA ligase 4 expression in the resistant RHUT78 and RMEC1 lines but was not a consistent finding in repeat experiments (**Fig 20a**). The expression of XRCC4 protein, in contrast was robust in all the cell lines (**Fig 20b**).

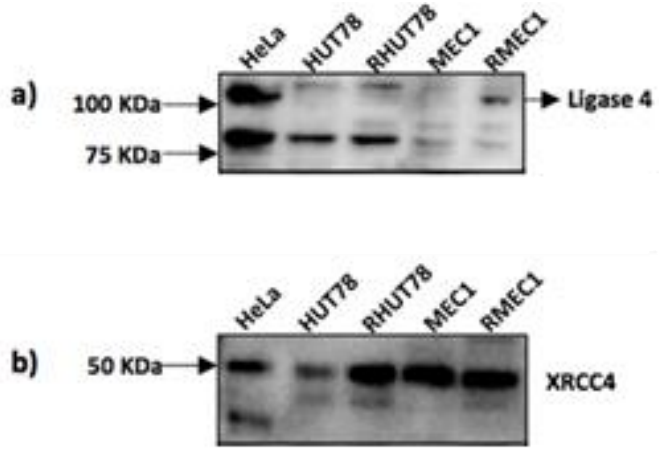

Figure 20: Western blot analysis of downstream NHEJ proteins in a variety of cell lines. 10 µg of protein from HeLa, (parental) HUT78, MEC1, and (resistant) RHUT78 and RMEC1 whole cell lysates was loaded on to the gel and after transferring the proteins onto a PVDF membrane, was probed with a). Ligase 4 (1:1600) and b) XRCC4 (1:2000) antibodies. Expected protein sizes for both the antibodies are Ligase 4: 109 kDa and XRCC4: 50 kDa. The bands appearing around 75 kDa for Ligase 4 could be non-specific.Equal amount of protein was loaded on to the gel as determined by Bio-Rad *DC* Protein Assay kit.

3.5 Analysis of the expression of Ligase 4 and XRCC4 proteins in CLL patient samples

A random cohort of CLL cases were chosen to investigate the expression of Ligase 4 and XRCC4 proteins by immunoblotting. The expression of Ligase 4 was variable in this cohort and was

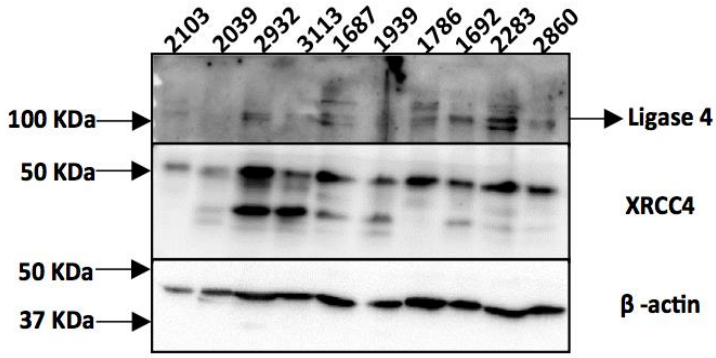

Figure 21: Verifying the protein expression of Ligase 4 and XRCC4 in CLL cases. 10 µg whole cell lysate from CLL cells were loaded on to a gel and the proteins transferred onto a PVDF membrane. The membrane was probed with Ligase 4 antibody (1:1600 dil), expected protein size 109 kDa, XRCC4 antibody (1:2000 dil), expected protein size 50 kDa. The blot was later probed with beta actin antibody (1:10000 dil), which was used as a loading control.

detected only in a subset of cases 2932, 2860,1687,1786, 1692 and 2283 (**Fig 21**). The cases 2932 and 2860 had a genetic abnormality in the form of a deletion 11q22. In contrast, XRCC4 expression was detected more widely across all the CLL cases.

3.6 Analysis of the effects of irradiation on expression of Ligase 4, XRCC4 and p53 proteins

In order to understand the effects of irradiation on the expression of

Ligase 4, XRCC4 and p53, MEC1 and HeLa cell lines were chosen as both show good expression of wild type p53 [146]. HeLa cells served as a positive control for Ligase 4 expression. The cell lines were cultured and exposed to two different doses of irradiation, 3 Gy and 5 Gy. Cells were harvested at 3, 6 and 24 hours and cell lysates prepared. Immunoblotting was carried out to determine the expression of the above mentioned proteins. In the MEC1 cell line, there was no significant change in expression of Ligase 4 protein upon exposure to the two different grades of irradiation when compared to untreated controls at the different time points. In contrast, in the HeLa cell line, Ligase 4 expression was comparitively more prominent than in untreated controls at both grades of irradiation and time points (**Fig 22a**). There was less variability in XRCC4 protein expression in both irradiated and untreated lysates upto 24 hours in both MEC1 and HeLa cell lines (**Fig 22b**). The expression of p53 expression, which was used as a positive control as it is reported to be higher in irradiated samples was detected strongly across all MEC1 lysates but not in the HeLa lysates. Only faint bands were visualised in HeLa cells and be a reflection of the batch of HeLa cells used[147]. The experiment was repeated to study the effects of longer incubation times after irradiation to see if the expression of Ligase 4 protein was altered (see **Fig 23**).

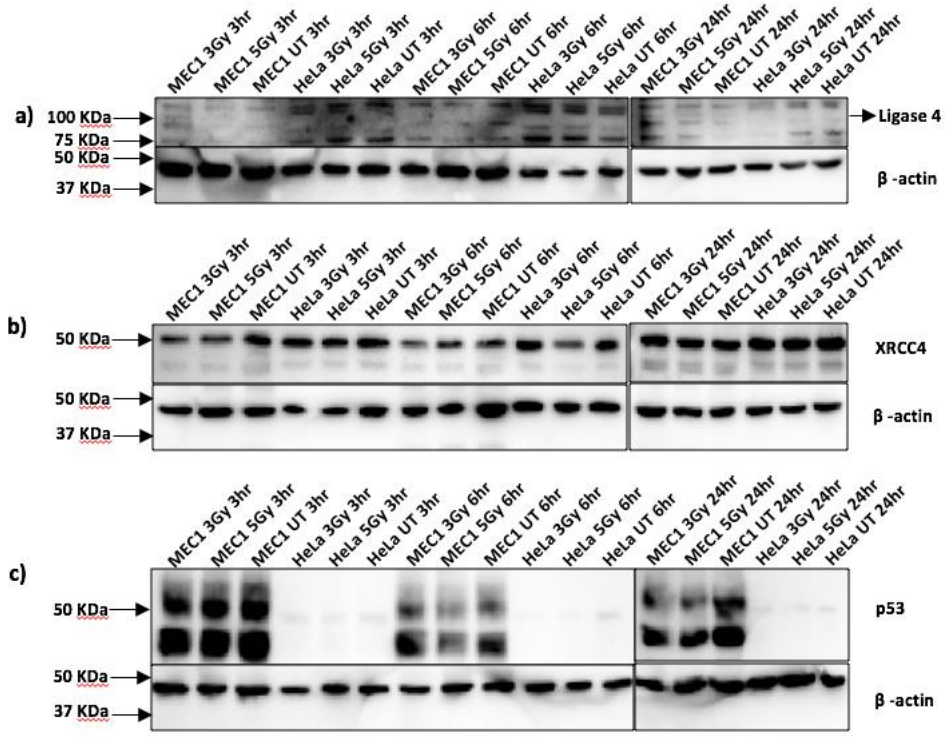

Figure 22(a, b and c): Effect of IR (3 Gy and 5 Gy) after 3, 6 and 24 hours on DNA Ligase 4, XRCC4 and p53 expression in HeLa and MEC1 cells. 10 µg of protein generated from irradiated HeLa and MEC1 cells harvested at different time points (3, 6 and 24 hours), were loaded on to a gel and after transferring the proteins onto a PVDF membrane, the membrane was probed with **a)** Ligase 4 antibody (1:1600), **b)** XRCC4 antibody (1:2000), and **c)** p53 antibody (1:1000). The blot was later probed with beta actin antibody.

The Ligase 4 protein expression in MEC1 cells treated with both 3 Gy and 5 Gy at 48 hours, was higher when compared to untreated control (**Fig 23a**). Changes in Ligase 4 expression in HeLa cells on irradiation were less prominent at all time points (**Fig 23a**). There was less variability in XRCC4 protein expression in both treated and untreated samples across all the three time points (**Fig 23b**).

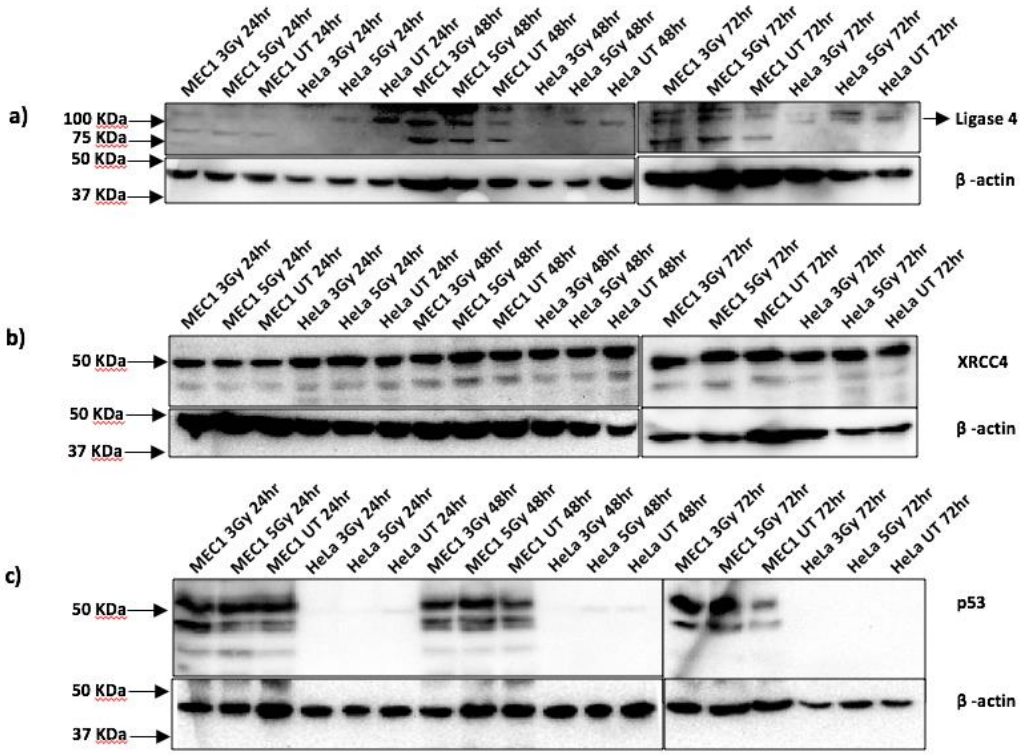

Figure 23 (a, b and c): Effect of IR (3 Gy and 5 Gy) after 24, 48 and 72 hours on DNA Ligase 4, XRCC4 and p53 expression in HeLa and MEC1 cells. 10 µg of protein generated from irradiated HeLa and MEC1 cells harvested at different time points (24, 48 and 72 hours) were loaded on to a gel and after transferring the proteins onto a PVDF membranes, probed with a) Ligase 4 antibody (1:1600 dil, 109 kDa), b) XRCC4 antibody (1:2000 dil, 50 kDa) (23b) and c) p53 antibody (1:1000 dil), 53 kDa). The blot was later probed with beta actin antibody (1:10000dil).

Expression of p53 protein seemed to be slightly higher in irradiated MEC1 cells at 48 hours and 72 hours with a dose of 5 Gy irradiation compared to the non-irradiated controls (**Fig 23c**). There were no clear changes in p53 expression in MEC1 cells (**Fig 23c**).

3.7 Analysis of the effects of irradiation and SCR7 on growth and survival in haematopoietic cell lines

For these studies, MEC1 and Daudi cells were treated with 5 Gy of irradiation and additionally exposed to the DNA ligase 4 inhibitor, SCR7, at defined concentrations of the drug as previously described[124]. Cytotoxicity was measured using a PI and DiOC6 assay by flow cytometry and the percentage of live cells was calculated at different time intervals (24, 48 and 72 hours). As shown for Daudi cells (**Fig 24)**, upon irradiation alone, the percentage of live cells dropped by 15.13 % at 24 hours, 30.15 % at 48 hours and 30.47 % at 72 hours (data described in appendix). Treatment with SCR7 alone at concentrations up to 100 µM, had no significant effect on cell viability. Upon exposure to a 250 µM of the drug, the percentage of live cells decreased by 32.88 % at 72 hours. In contrast, upon the combined treatment with irradiation and drug, there was a decrease in the percentage of live cells for all concentrations when compared to untreated control. At 24 hours for 10 µM, 50 µM and 100 µM inhibitor concentrations, there was slight decrease in the percentage of live cells by 15.69 %, 16.14 % and 18.79 % in cells treated with combination of irradiation and drug when compared to treatment with drug alone. For cells treated with irradiation and SCR7 inhibitor (50 µM and 100 µM), at 72 hours the percentage of live cells dropped by 27.55 % and 39.17 % when compared to cells treated with the inhibitor

only. Lastly, at 250 µM concentration, there was a narrow difference in percentage of live cells between cells treated with drug alone and in combination with drug and irradiation by 3.76 %, 18.82 % and 11.81 % at 24 hours, 48 hours and 72 hours respectively. In summary, only high concentrations of inhibitor had a significant effect on cell viability.

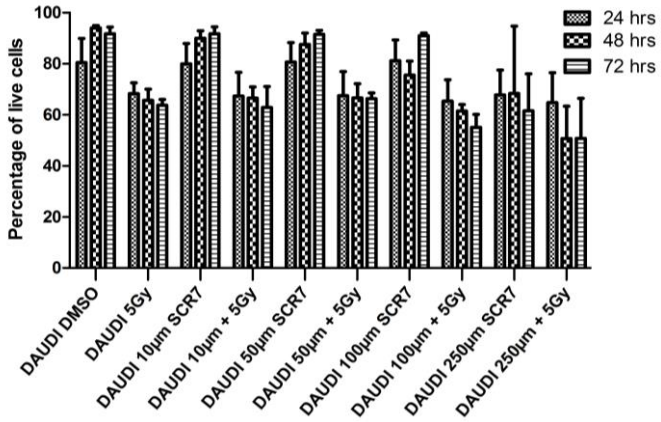

Figure 24: Assessment of cytoxicity in Daudi cells on treatment with irradition and/or SCR7. Bar graphs showing the percentage of live Daudi cells after treatment with 5 Gy irradiation (IR) followed by treating with varied concentrations (10 µM, 50 µM, 100 µM, 250 µM) of the *LIG4* inhibitor SCR7. The percentages of live cells were measured at 24 hours, 48 hours and 72 hours respectively. Error bars represent standard deviation from three independent experiments.

In addition to the above experiments on Daudi cells, MEC1 cells were also investigated for the effects of irradiation and SCR7. There was no change in cell viability at all time points upon treatment with drug alone (10 µM, 50 µM and 100 µM) as shown in (**Fig 25)**.

Sample name and treatment (IR=5Gy)	Percentage of dead cells (%)		
	24 hours	48 hours	72 hours
Daudi IR	15.13	30.15	30.46
MEC1 IR	15.80	32.29	29.82
Daudi 10 µM + IR	16.30	29.26	31.48
MEC1 10 µM + IR	19.08	29.92	41.33
Daudi 50 µM + IR	16.13	29.15	27.71
MEC1 50 µM + IR	18.43	27.59	41.03
Daudi 100 µM + IR	18.78	34.58	39.93
MEC1 100 µM + IR	16.81	27.13	40.24
Daudi 250 µM + IR	19.53	46.08	44.68
MEC1 250 µM + IR	28.21	35.01	70.69

Table 5: Percentage of dead cells in MEC1 and Daudi cell lines under various treatment conditions with SCR7 and 5 Gy IR.

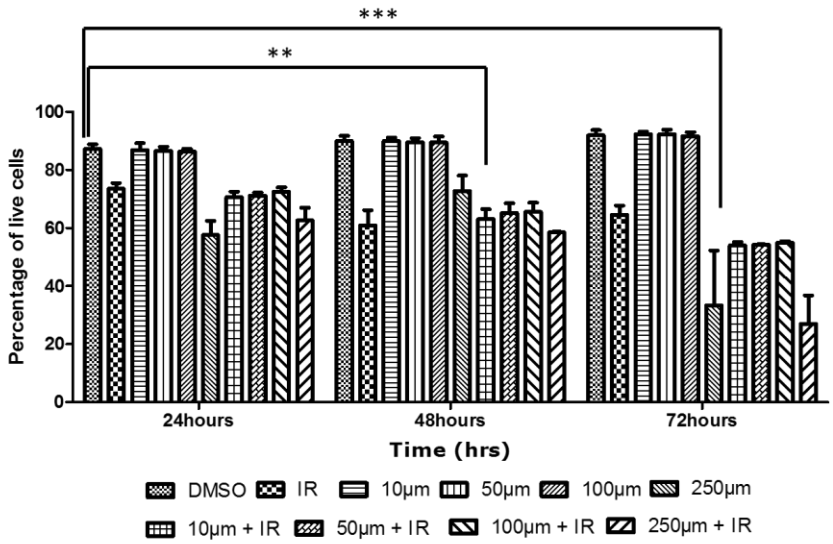

Figure 25: Assessment of cytotoxicity in MEC1 cells following exposure to irradiation and/or SCR7. Bargraphs showing the percentage of live MEC1 cells upon treatment with 5 Gy irradiation (IR) followed by treating with varied concentrations (10 µM, 50 µM, 100 µM, 250 µM) of *LIG4* inhibitor SCR7. The percentage of live cells were measured at different time points 24, 48 and 72 hours using flow cytometric assessment of PI and DiOC6 staining. Statistical analysis was performed using Two way anova, P value > 0.05. Error bars represent standard deviation from three independent experiments.

The percentage of cell death increased upon treatment with 250 µM of inhibitor alone and in combination with irradiation by 34.02 %,19.22 % (inhibitor only) and 28.21 %, 35 % (inhibitor with IR) at 24 hours and 48 hours respectively. The percentage of live cells at 250 µM decreased by 63.73 % and 70.69 % for both the samples treated with inhibitor alone and in combination with irradiation at 72 hours. The percentage of cell death in MEC1 is visibly higher at 72 hours for all combinations of drug and irradiation when compared to that of Daudi cells as shown in (**Table 5)**.

3.8 Analysis of the sensitivity of leukemic cells to irradiation following pre-treatment with SCR7 inhibitor

To assess the radiosensitivity of Daudi and MEC1 cells, two concentrations of SCR7 (10 µM and 100 µM) were used prior to irradiation. After 24 hours of treatment, the cells were exposed to 5 Gy irradiation and were harvested at 48 hours and 72 hours and the percentage of live cells was determined using flow cytometry. The percentage of live cells in treated samples was compared to untreated control samples (i.e no irradiation or drug). The percentage of live Daudi cells did not vary for 10 µM concentration of drug alone at both 48 and 72 hours whereas it decreased by 6.9 % and 4.4 % for 100 µM concentration at 48 and 72 hours. The percentage of cell death in

Daudi cells at 48 hours after treatment with irradiation was 19.7 %, 19.3 % (10 µM and 100 µM) and 19.5 %, 17.2 % (10 µM and 100 µM) at 72 hours on comparison with untreated control samples (**Fig 26**). The cell death percentage pattern seems to be quite similar for both concentrations and timepoints suggesting that the cells were not sensitized to irradiation at these concentrations of the inhibitor treatment. Similar to Daudi cells, there was no noticeable change in decrease of percentage of live cells at both concentrations (10 µM and 100 µM) and time points upon treatment with inhibitor alone when compared to untreated control in MEC1 cells.

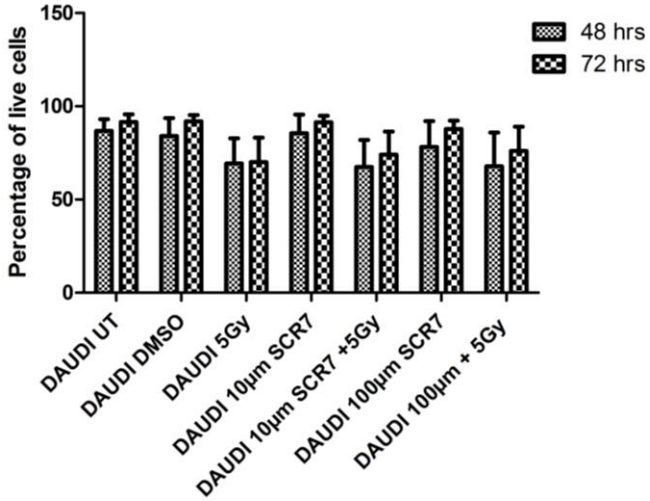

Figure 26: Assessment of radiosensitivity assay of Daudi cells on pre-treatment with SCR7. Bargraphs showing the percentage of live Daudi cells upon pre-treatment with varied concentrations (10 µM and 100 µM) of *LIG4* inhibitor SCR7 for 24 hours followed by 5 Gy irradiation to measure the sensitivity of cells to irradiation. The percentages of live cells was measured at 48 and 72 hours using staining with PI and DiOC6 and flow cytometry. Error bars represent standard deviation from three independent experiments.

The percentages of cell death in MEC1 cells at 48 hours after treatment with irradiation was 13.3 %, 14.4 % (10 µM and 100 µM) and 7 %, 12.5 % (10 µM and 100 µM) at 72 hours when compared with untreated control samples (**Fig 27**). Analysis of the percentage of live cells in both the cell lines suggests that Daudi cells were more slightly more responsive to the inhibitor and irradiation treatment as compared to MEC1 cells.

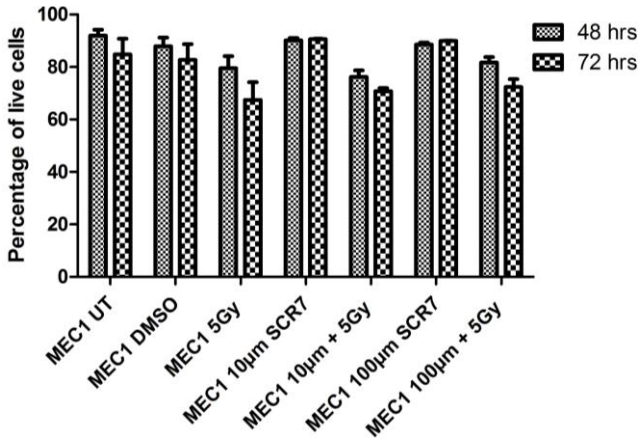

Figure 27: Assessment of radiosensitivity of MEC1 cells pre-treated with SCR7. Bar graph showing the percentage of live MEC1 cells upon treatment with varied concentrations (10 µM and 100 µM) of SCR7 prior to 5 Gy irradiation to measure the sensitivity of cells to IR. The percentages of live cells were measured at 48 and 72 hours as previously described. Error bars represent standard deviation from three independent experiments.

3.9 Investigation of effects on cell proliferation upon treatment with SCR7 inhibitor and irradiation

To further understand the effects of SCR7 on cells, cell proliferation was measured using a BrdU assay (Roche, UK). The assay was

performed with HeLa, Daudi and MEC1 cell lines. The cells were treated with different concentrations (10 µM, 50 µM, 100 µM and 250 µM) of inhibitor alone and also in combination with irradiation. Cells devoid of any SCR7 in the medium and only exposed to irradiation (5 Gy) were used as controls. The proliferation was measured at 24, 48 and 72 hours. The HeLa cells at 24 hours showed a low level of proliferation in all samples irrespective of treatment (**Fig 28**). The proliferation rate seemed to be enhanced at 48 hours in cells treated with inhibitor alone. At 10 µM and 50 µM concentrations, the proliferation was low compared to the untreated control, however, at 100 µM and 250 µM concentrations the cell growth was on par with the untreated control sample. In the samples treated with inhibitor and irradiation at 48 hours, the cell growth rate for all concentrations except 50 µM and 100 µM, showed similar rates of proliferation as that of the untreated controls. However, in samples treated with 50 µM and 100 µM concetrations of inhibitor and 5 Gy IR, there was a slight decrease in proliferation as shown in (**Fig 28**). At 72 hours the cell proliferation was highest and consistent among all samples. Indeed, cells treated with high doses of inhibitor (100 µM and 250 µM) and irradiation, showed a slight enhancement of cell proliferation when compared to untreated controls. In MEC1 cells the proliferation goes down at 24 hours in all treated and untreated samples. The cell

proliferation improves at 48 hours as compared to 24 hours across all the samples (**Fig 29**). At 48 hours, the proliferation of cells treated with inhibitor (10 µM, 50 µM, 100 µM, 250 µM) alone was high when compared to cells treated with a combination of inhibitor and irradiation. The samples treated with both the inhibitor and the irradiation had diminished cell proliferation compared to the untreated control samples at 48 hours (**Fig 29**).

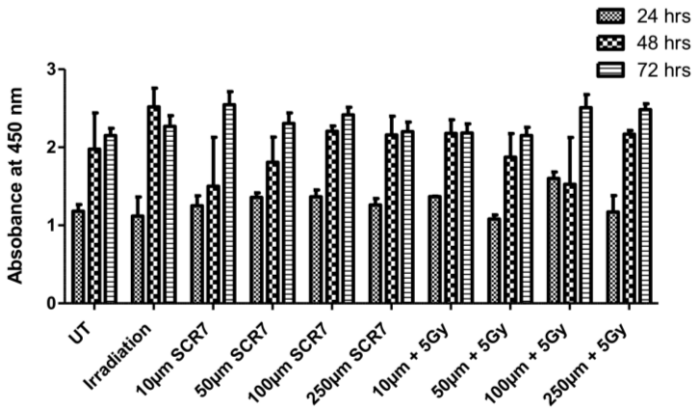

Figure 28: Results of a BrdU assay to assess cell proliferation of HeLa cells subjected to IR and SCR7 inhibitor. Bar graph showing the change in absorbance after treatment with varied concentrations (10 µM, 50 µM, 100 µM, 250 µM) of Ligase 4 inhibitor SCR7 alone and in combination with irradiation (IR, 5 Gy). The proliferation was measured at 24 hours, 48 hours and 72 hours. Error bars represent standard deviation from three independent experiments.

At 72 hours the cell proliferation pattern was very similar to that at 48 hours. However, at certain concentration of inhibitor (100 µM) and irradiation, the cell proliferation decreased visibly when compared to the untreated control. Neither MEC1 and HeLa cell proliferation seems to be affected ‘significantly’ by SCR7 inbitor treatment alone or in

combination with irradiation. In contrast, Daudi cells had a better response to inhibitor and irradiation treatment in terms of decreased cell proliferation. In Daudi cells, the rate of cell proliferation decreased gradually at high concentrations with inhibitor treatment alone (50 µM, 100 µM, 250 µM) at 48 hours when compared to untreated control (**Fig 30**). At 72 hours it was observed that Daudi cells treated with a high dose of inhibitor (250 µM) had reduced cell proliferation when compared to controls.

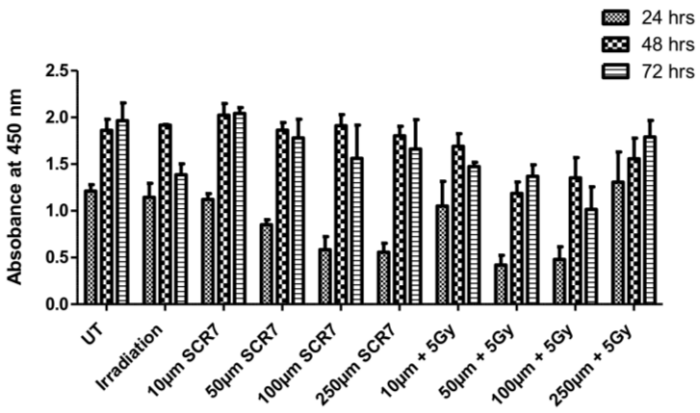

Figure 29: BrdU assay measuring cell proliferation of MEC1 cells upon subjection to IR and SCR7 inhibitor. Bar graph showing the change in absorbance of HeLa cells upon treatment with varied concentrations (10 µM, 50 µM, 100 µM, 250 µM) of Ligase 4 inhibitor SCR7 alone and in combination with irradiation (IR, 5 Gy). Error bars represent standard deviation from three independent experiments.

Treatment of cells in combination with irradiation at all concentrations of the inhibitor resulted in lower rates of proliferation upon comparison with untreated cells at the all the time points suggesting that the

inhibitor along with irradiation has an additive effect on cell proliferation in Daudi cells.

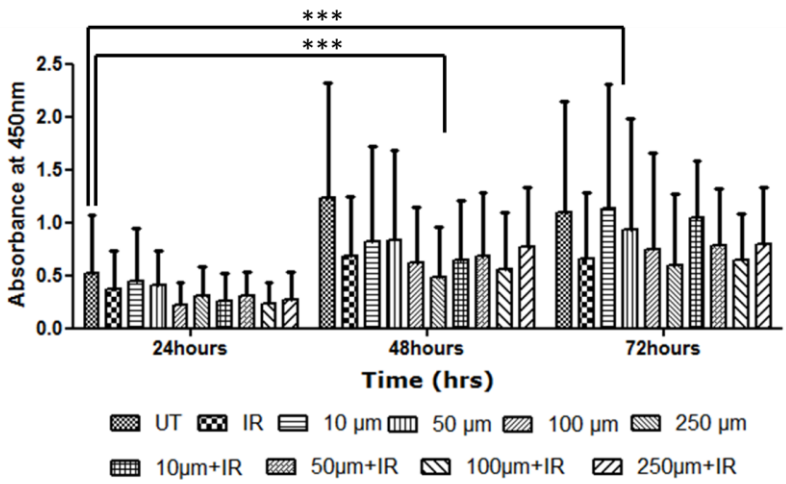

Figure 30: BrdU assay measuring cell proliferation of Daudi cells upon exposure to IR and SCR7 inhibitor. Bar graph showing the change in absorbance values of HeLa cells upon treatment with varied concentrations (10 µM, 50 µM, 100 µM, 250 µM) of Ligase 4 inhibitor SCR7 alone and in combination with irradiation (IR, 5 Gy). The proliferation was measured at 24 hours, 48 hours and 72 hours. Statistical analysis was performed using Two way anova, P value >0.0001 for three independent experiments. Error bars represent standard deviation from three independent experiments.

Chapter 4: Discussion

Several studies have focused on the role of DNA ligases in cancer[148-150]. Two DNA ligases have been shown to be over expressed in cancers, DNA Ligase 1 in breast, lung, ovarian, sarcoma and neuroblastoma and DNA Ligase 3α in chronic myeloid leukemia[148,149]. Recent studies show that *LIG4* gene expression is downregulated in 51 % of colorectal cancers due to abnormal promoter methylation activity[151]. Altered expression of the three DNA ligases has been associated with genetic instability[44].

One of the main aims of the project was to understand the role of DNA ligases in lymphoid malignancies. PCR Primers were designed to amplify *LIG1, LIG3* and *LIG4* mRNA and intial experiments were performed to identify optimal annealing temperature for each primer set using cDNA derived from K562 and MEC1 cell lines. Once optimised, the primers were used to determine the presence or absence of the ligases in CLL cases (**Figs 16 & 17**). Endpoint PCR experiments confirmed the expression of *LIG1, LIG3 and LIG4* in a small cohort of randomly chosen CLL cases and the HS-5 cell line (Bone Marrow stromal cell line).

Our studies were mainly focussed on the expression of the Ligase 4 protein in Chronic Lymphocytic Leukemia. Interestingly, deficiency and mutations of Ligase 4 has been associated with *LIG4* syndrome (as discussed in introduction), where patients are sensitive to irradiation and have increased risk of developing leukemia[152]. Initial experiments to asses the presence or absence of Ligase 4 protein, was done with a Ligase 4 antibody from Protein tech, UK (12695-1-AP). The protein was detected in the HeLa cell line (positive control) and also in MEC1, Daudi and HUT78 cell lines (**Fig 18**). These results were later confirmed using a second Anti-DNA Ligase IV antibody (ab26039) from Abcam, UK. The presence of Ligase 4 was detected in the positive control cell line, HeLa, and also MEC1 cell line, whereas in other cell lines such as Daudi and K562, protein could not be detected. (**Fig 19**). These discrepancies will have to further be analysed carefully to make solid conclusions from these studies. Nevertheless, one of the several reasons for the absence of Ligase 4 in certain cell lines might be due to changes in the extent of ongoing DNA damage, which might further activate the NHEJ pathway and result in a reduced need for Ligase 4 protein expression.

HDACIs have been known to cause DNA damage and studies have shown that treatment with HDACIs increases the frequency of NHEJ

pathway[145]. ATPase Family AAA Domain Containing 5 (ATAD5), is a biomarker for identifying genotoxic compounds, its protein levels are known to increase upon increase in DNA damage[153]. Using an ATAD5 luciferase assay, certain HDACIs were identified to cause potent DNA damage by inducing ROS[153]. Studies show that HDACI drugs escalate the NHEJ frequency because of the generation of DNA damage in the form of DSBs as observed in human cell lines. HDACIs did not show any specific changes in HR but did generate cellular resistance to HDACIs by keeping the cells alive[145]. Romidepsin is a HDACI which is licensed drug for treatment cutaneous T cell lymphomas[144]. Hence, Romidepsin resistant cell lines, such as RMEC1 and RHUT78, and wild type MEC1 and HUT78 cell lines were used to study ligase 4 expression. Ligase 4 protein activity was low in the RMEC1 cell line and was not detected in RHUT78 cell line suggesting that the resistant cells, due to continuous exposure to the drug might have undergone chromatin remodelling, affecting the cellular signalling pathways (p21)[154] thereby masking the Ligase 4 protein activity **(Fig 20a)**.

We also investigated the expression of another critical NHEJ protein, XRCC4. This protein works in unison with Ligase 4 during ligation of DNA strands[61]. XRCC4 protein expression was detected in all cell types used with very little variability. Further studies were focussed on

understanding the the influence of irradiation on Ligase 4 and XRCC4 protein expression . We hypothesised that irradiation might induce DNA damage as radiation energy is directly absorbed by the DNA resulting in ionisation and breakage of the DNA strand. This should then trigger increased protein expression of Ligase 4 and XRCC4 which are involved in the NHEJ pathway[3,155]. The amount of irradiation is directly proportional to the amount of DSBs produced[156]. The studies were carried out on MEC1 and HeLa cells at two different doses of irradiation (3 Gy and 5 Gy) over a range of incubation times (3, 6, 24, 48 and 72 hours)[157]. Ligase 4 and XRCC4 protein expression was detected consistently across untreated and treated samples (**Fig 22 & 23**). Simultaeneously, p53 protein expression was measured as an irradiation control[146,147]. This was detected in the MEC1 cell line but was very faint in the HeLa cell line.

p53 protein disruption leads to a variety of cancers[158,159] and studies have also shown that cells exposed to IR have increased amount of p53 expression which in turn leads to apoptosis[147]. From the results obtained we could not form any meaningful conclusions as there was no significant change in Ligase 4 expression upon exposure to irradiation in MEC1 and HeLa cell lines. This may be due to high levels of radioresistance or alternate pathways of DNA repair. In the time

frame of the project it was not possible to quantitatively assess DSBs following irradiation. Interestingly, the HeLa cell line, which served as the positive control for Ligase 4 expression, had comparitively brighter bands when compared to MEC1 cells.

There was no significant change in XRCC4 protein expression. A previous study described the expression of DNA repair proteins Ligase 4, XRCC4 and Ku 70/80 in human fibroblast cell lines derived from cancer patient samples who have undergone radiotherapy[160]. In this study, no significant difference (< 2 fold) was found upon comparing the protein expressions of Ligase 4, XRCC4, Ku 70/80 and DNA-PK$_{cs,}$ thereby not showing much variation of expression among different samples[160].

Studying the expression of Ligase 4 and XRCC4 proteins in a random cohort of CLL patient samples suggests that Ligase 4 expression is variable in individual cases and may be worth pursuing to understand the significance and causes. XRCC4 expression, in contrast was ubiquitous and showed less variability cases 2932 and 2283 which showed Ligase 4 expression also had 11q22 deletion (Appendix) suggesting that such expression might be due to ongoing DNA damage. Some other cases which showed positive expression did not

have any common or specific genetic abnormalities in their clinical profile. Generation of more meaningful and definite conclusions will require a large cohort of samples with well defined clinical, genetic data and outcomes.

Several studies indicate that disruption of the *LIG4* gene results in the cells having increased sensitivity to ionising irradiation (as discussed in introduction)[150]. In addition to this, *LIG4* has a key role in NHEJ and this pathway plays a major role in the development of resistance in cancer cells to radiation and chemotherapeutic drugs[107]. SCR7 is a compound that acts as an inhibitor of *LIG4* and there is a suggestion that it can be used therapeutically[124]. SCR7 has high binding energy (-29.14 kcal/mol) to the DBD of Ligase 4 protein thereby disturbing its binding capacity to DSBs. Docking studies show that the binding of SCR7 inhibitor to the Ligase 4 protein leads to a loss of hydrogen bond interactions between the Ligase 4 DBD and DNA[124]. This disruption results in the acumulation of DSBs thereby resulting in cytotoxicity in certain cell lines like Nalm6, a B cell precursor leukemia cell line[124].

Another aspect of our study was to study the effects of a newly designed inhibitor of the NHEJ pathway, SCR7, on leukemic cell lines[124]. Using methods already published[124], we tried to measure the cytotoxicity, radiosensitivity and effect on cell proliferation of leukemic cell lines (Daudi and MEC1) after treatment with SCR7 inhibitor. Whilst investigating the cytotoxicity, the cell death increased by 32.88% in Daudi cells and 63.73% in MEC1 cells at very high concentration of 250 µM of inhibitor alone (**Fig 24 & 25**) at 72 hours. Whereas at 24 and 48 hours, the difference in cell death percentages were comparitively low. The reason behind elevated cell death may be attributed to exposure of cells to high doses of the drug rather than DNA damage as the percentage of cell death measured at 72 hours with and without irradiation in presence of SCR7 is abnormally high.

We assesed if the Daudi and MEC1 cell lines could be sensitised to irradiation by treating them first with the SCR7 inhibitor (10 µM and 100 µM) followed by irradiation (5 Gy) (**Fig 26 & 27**). We narrowed down the inhibitor concentration based on the previous results from cytotoxicity experiments which showed they did not result in rapid cell death (**Fig 24 & 25**). It has previously been suggested that treatment with SCR7 followed by irradiation results in radiosensitivity and apoptosis[124]. In our study, cell death after irradiation treatment was

observed but in combination with SCR7, there was no significant change in cell death at varied time points in either Daudi and MEC1 cells (**Fig 26 & 27**) implying that SCR7 treatment did not radiosensitise the cells effectively. Previous studies were performed on mouse models of breast adenocarcinoma where there was a 4 fold increase in the life span of animals treated with SCR7[124], whereas in the Dalton Lymphoma mouse model, there was no change a in tumour growth or life span, which may explain our observation in leukemic and lymphoma cell lines. Cell proliferation assays carried out on MEC1, Daudi and HeLa cells showed that irradiation in combination with SCR7 inhibitor didn't not have any potent effect on the proliferation of both HeLa and MEC1 cells (**Fig 28 and 29**). Only Daudi cells(**Fig 30**) had stunted proliferation rates when compared to their untreated controls suggesting that SCR7 inhibitor along with irradiation interfered with the cell cycle pattern.

Future work

In order for better understanding of ligase 4 expression, it will be crucial to measure the gene expression of *LIG4* in cell lines and primary cells by qPCR, and also upon treatment of irradiation to see whether the exposure triggers an increase in DNA repair thereby upregulating *LIG4* expression. Gene expression of *LIG4* by qPCR in a wider cohort of CLL patient samples with defined genetic abnormalities

and who have undergone chemotherapeutic treatment may provide further insights. These set of experiments will enable us to understand if genetic abnormalities and chemotherapy affect the DNA repair processes in CLL patients. Lastly, it would be important to investigate the cytoxic or radiosensitising effects of the SCR7 drug on cells with parallel assays that allow quantitative estimation of DSBs to allow meaningful correlations and it is possible that other existing novel inhibitors of critical proteins in the DNA repair pathways may still be relevant in the treatment of Chronic Lymphocytic Leukemia and indeed other haematological malignancies.

Appendix

Sample	WBC	Rai	Binet	p53	Karyotype	Treated
2270	90	0	A		-	-
2256	51.1	I	B	B	17p13	yes
3007	241.2	-	A	-	-	-
3314	359.8	II	B	-	-	-
3147	217.3	-	-	-	-	-
2103	125	0	A	-	17p13	-
2039	10.1	-	-	-	11q22	-
2932	175.7	II	B	-	11q22	-
3113	172.4	-	B	-	-	-
1687	656	IV	C	-	-	-
1939	624		-	C	-	yes
1786	110	IV	B	-	-	yes
1692	300	III	C	B	-	yes
2283	326	I	A	-	11q22	yes
2860	63.2	-	B	-	normal	yes

Table 6: Clinical data of all the CLL patients used in the project.

Sample	Percentage of live cells			Percentage of live cells		
	48 hours	48 hours(repeat)	Normalized values to DMSO	72 hours	72 hours(repeat)	Normalized values to DMSO
DAUDI DMSO	74.3	93.7		88.5	95.3	
DAUDI 5Gy	55.8	82.86	82.5	56.9	83.2	76.2
DAUDI 10µm SCR7	75.5	95.5	101.8	87.9	94.95	99.5
DAUDI 10µm SCR7 +5Gy	52.9	82	80.3	61.6	86.4	80.5
DAUDI 100µm SCR7	64.4	92	93.1	83.4	92.3	95.6
DAUDI 100µm + 5Gy	49.7	85.9	80.7	63.1	89	82.8
MEC1 DMSO	84.5	91.19		88.7	76.76	
MEC1 5Gy	75	84.14	90.6	74.2	60.65	81.50
MEC1 10µm SCR7	89.2	91	102.6	90.8	90.37	109.49
MEC1 10µm + 5Gy	73.6	78.74	86.7	69.6	71.99	85.57
MEC1 100µm SCR7	87.8	89.28	100.8	90	89.91	108.73
MEC1 100µm + 5Gy	79.7	83.75	93.0	69.4	75.37	87.49

Table 7: Raw data of radiosensitivity assay as shown in (Figures 26 and 27)

Sample	Percentage of live cells			Percentage of live cells			Percentage of live cells		
	24 hours	24 hours (repeat)	Normalised values to DMSO	48 hours	48 hours (repeat)	Normalised values to DMSO	72 hours	72 hours (repeat)	Normalised values to DMSO
DAUDI DMSO	71	89		94.88	93		89	94.3	
DAUDI 5Gy	64	72	84.87	61.24	70	69.85	66	61.46	69.53
DAUDI 10µm SCR7	72	87	99.38	92.85	87	95.72	89	94.4	100.05
DAUDI 10µm + 5Gy	58	76	83.69	70.91	62	70.74	71	54.6	68.52
DAUDI 50µm SCR7	73	88	100.26	91.97	83	93.12	93	90	99.83
DAUDI 50µm + 5Gy	58	76	83.86	72.11	61	70.84	64	68.5	72.28
DAUDI 100µm SCR7	73	89	100.88	70.06	81	80.40	92	89.9	99.23
DAUDI 100µm + 5Gy	57	73	81.21	58.92	64	65.42	50	60.1	60.06
DAUDI 250µm SCR7	58	77	84.23	94.68	42	72.74	47	76.04	67.12
DAUDI 250µm + 5Gy	53	76	80.47	63.31	38	53.92	35	66.4	55.31
MEC1 DMSO	90	84		93.00	86.85		95.00	88.90	
MEC1 5Gy	77	70	84.32	70.00	51.78	67.71	59.00	70.07	70.18
MEC1 10µm SCR7	91	82	99.60	92.00	87.87	100.01	94.00	90.50	100.33
MEC1 10µm + 5Gy	74	67	80.92	69.00	57.04	70.08	56.00	51.90	58.67
MEC1 50µm SCR7	89	84	99.31	92.00	86.98	99.52	95.00	89.70	100.44
MEC1 50µm + 5Gy	73	69	81.57	71.00	59.23	72.41	54.00	54.45	58.97
MEC1 100µm SCR7	88	84	98.96	93.00	85.85	99.44	94.00	89.30	99.67
MEC1 100µm + 5Gy	75	70	83.19	71.00	60.05	72.87	54.00	55.90	59.76
MEC1 250µm SCR7	49	66	65.98	82.00	63.29	80.78	0.60	66.10	36.27
MEC1 250µm + 5Gy	55	70	71.79	59.00	57.89	64.99	10.00	43.90	29.31

Table 8: Raw data values of cytotoxicity assays for Daudi and MEC1 cells at 24 , 48 and 72 hours (Figure 24 & 25).

References

1. Hoeijmakers JH. Genome maintenance mechanisms for preventing cancer. *Nature*. 2001;411(6835):366-374.

2. Friedberg EC, Walker GC, Siede W. *DNA repair and mutagenesis (2nd edition).* Washington, DC, USA: ASM Press; 2005.

3. Ward J. DNA damage produced by ionizing radiation in mammalian cells: Identities, mechanisms of formation, and reparability. *Prog Nucleic Acid Res Mol Biol*. 1988;35:95-125.

4. Sonntag C. *The chemical basis of radiation biology.* Taylor & Francis London; 1987.

5. Riley P. Free radicals in biology: Oxidative stress and the effects of ionizing radiation. *Int J Radiat Biol*. 1994;65(1):27-33.

6. Siddiqi MA, Bothe E. Single-and double-strand break formation in DNA irradiated in aqueous solution: Dependence on dose and OH radical scavenger concentration. *Radiat Res*. 1987;112(3):449-463.

7. Cooke MS, Evans MD, Dizdaroglu M, Lunec J. Oxidative DNA damage: Mechanisms, mutation, and disease. *FASEB J*. 2003;17(10):1195-1214.

8. Lindahl T. Instability and decay of the primary structure of DNA. *Nature*. 1993;362(6422):709-715.

9. Aguilera A, Gómez-González B. Genome instability: A mechanistic view of its causes and consequences. *Nature Reviews Genetics*. 2008;9(3):204-217.

10. Christmann M, Tomicic MT, Roos WP, Kaina B. Mechanisms of human DNA repair: An update. *Toxicology*. 2003;193(1):3-34.

11. Lindahl T. New class of enzymes acting on damaged DNA. . 1976.

12. Wilson III DM, Barsky D. The major human abasic endonuclease: Formation, consequences and repair of abasic lesions in DNA. *Mutat Res /DNA Repair*. 2001;485(4):283-307.

13. Frosina G, Fortini P, Rossi O, et al. Two pathways for base excision repair in mammalian cells. *J Biol Chem*. 1996;271(16):9573-9578.

14. Hanawalt PC. Subpathways of nucleotide excision repair and their regulation. *Oncogene*. 2002;21(58):8949-8956.

15. Mellon I, Spivak G, Hanawalt PC. Selective removal of transcription-blocking DNA damage from the transcribed strand of the mammalian DHFR gene. *Cell*. 1987;51(2):241-249.

16. Evans E, Moggs JG, Hwang JR, Egly JM, Wood RD. Mechanism of open complex and dual incision formation by human nucleotide excision repair factors. *EMBO J*. 1997;16(21):6559-6573.

17. de Laat WL, Appeldoorn E, Sugasawa K, Weterings E, Jaspers NG, Hoeijmakers JH. DNA-binding polarity of human replication protein A positions nucleases in nucleotide excision repair. *Genes Dev*. 1998;12(16):2598-2609.

18. de Laat WL, Jaspers NG, Hoeijmakers JH. Molecular mechanism of nucleotide excision repair. *Genes Dev*. 1999;13(7):768-785.

19. Hanawalt PC. Controlling the efficiency of excision repair. *Mutat Res /DNA Repair*. 2001;485(1):3-13.

20. Umar A, Kunkel TA. DNA-replication fidelity, mismatch repair and genome instability in cancer cells. In: *Ejb reviews 1996.* Springer; 1997:163-173.

21. Modrich P, Lahue R. Mismatch repair in replication fidelity, genetic recombination, and cancer biology. *Annu Rev Biochem*. 1996;65(1):101-133.

22. Fishel R, Lescoe MK, Rao M, et al. The human mutator gene homolog MSH2 and its association with hereditary nonpolyposis colon cancer. *Cell*. 1993;75(5):1027-1038.

23. Kunkel TA, Erie DA. DNA mismatch repair*. *Annu Rev Biochem*. 2005;74:681-710.

24. Christmann M, Tomicic MT, Roos WP, Kaina B. Mechanisms of human DNA repair: An update. *Toxicology*. 2003;193(1):3-34.

25. Genschel J, Bazemore LR, Modrich P. Human exonuclease I is required for 5' and 3' mismatch repair. *J Biol Chem*. 2002;277(15):13302-13311.

26. Helleday T, Lo J, van Gent DC, Engelward BP. DNA double-strand break repair: From mechanistic understanding to cancer treatment. *DNA repair*. 2007;6(7):923-935.

27. Johnson RD, Jasin M. Sister chromatid gene conversion is a prominent double-strand break repair pathway in mammalian cells. *EMBO J*. 2000;19(13):3398-3407.

28. Sonoda E, Takata M, Yamashita YM, Morrison C, Takeda S. Homologous DNA recombination in vertebrate cells. *Proc Natl Acad Sci U S A*. 2001;98(15):8388-8394.

29. New JH, Sugiyama T, Zaitseva E, Kowalczykowski SC. Rad52 protein stimulates DNA strand exchange by Rad51 and replication protein A. *Nature*. 1998;391(6665):407-410.

30. Park MS, Ludwig DL, Stigger E, Lee SH. Physical interaction between human RAD52 and RPA is required for homologous recombination in mammalian cells. *J Biol Chem*. 1996;271(31):18996-19000.

31. Liu N, Schild D, Thelen MP, Thompson LH. Involvement of Rad51C in two distinct protein complexes of Rad51 paralogs in human cells. *Nucleic Acids Res*. 2002;30(4):1009-1015.

32. Wiese C, Collins DW, Albala JS, Thompson LH, Kronenberg A, Schild D. Interactions involving the Rad51 paralogs Rad51C and XRCC3 in human cells. *Nucleic Acids Res*. 2002;30(4):1001-1008.

33. Thompson BJ, Camien MN, Warner RC. Kinetics of branch migration in double-stranded DNA. *Proc Natl Acad Sci U S A*. 1976;73(7):2299-2303.

34. Ip SC, Rass U, Blanco MG, Flynn HR, Skehel JM, West SC. Identification of holliday junction resolvases from humans and yeast. *Nature*. 2008;456(7220):357-361.

35. Makarova K, Aravind L, Koonin E. Holliday junction resolvases and related nucleases: Identification of new families, phyletic distribution and evolutionary trajectories. *Nucleic Acids Res*. 2000;28:3417-3432.

36. Constantinou A, Davies AA, West SC. Branch migration and holliday junction resolution catalyzed by activities from mammalian cells. *Cell*. 2001;104(2):259-268.

37. Holliday R. A mechanism for gene conversion in fungi. *Genet Res*. 1964;5(02):282-304.

38. Fugmann SD, Lee AI, Shockett PE, Villey IJ, Schatz DG. The RAG proteins and V (D) J recombination: Complexes, ends, and transposition. *Annu Rev Immunol*. 2000;18(1):495-527.

39. Roth DB. Restraining the v (d) j recombinase. *Nature Reviews Immunology*. 2003;3(8):656-666.

40. Roth DB. V (D) J recombination: Mechanism, errors, and fidelity. *Microbiology Spectrum*. 2014;2(6).

41. Lee GS, Neiditch MB, Salus SS, Roth DB. RAG proteins shepherd double-strand breaks to a specific pathway, suppressing error-prone repair, but RAG nicking initiates homologous recombination. *Cell*. 2004;117(2):171-184.

42. Martin IV, MacNeill SA. ATP-dependent DNA ligases. *Genome Biol*. 2002;3(4):REVIEWS3005.

43. Lehman IR. DNA ligase: Structure, mechanism, and function. *Science*. 1974;186(4166):790-797.

44. Ellenberger T, Tomkinson AE. Eukaryotic DNA ligases: Structural and functional insights. *Annu Rev Biochem*. 2008;77:313-338.

45. Howes TR, Tomkinson AE. DNA ligase I, the replicative DNA ligase. In: *The eukaryotic replisome: A guide to protein structure and function.* Springer; 2012:327-341.

46. Cooper GM, Hausman RE. *The cell.* Sinauer Associates Sunderland; 2000.

47. Tomkinson AE, Howes TR, Wiest NE. DNA ligases as therapeutic targets. *Translational cancer research*. 2013;2(3).

48. Levin DS, Bai W, Yao N, O'Donnell M, Tomkinson AE. An interaction between DNA ligase I and proliferating cell nuclear antigen: Implications for okazaki fragment synthesis and joining. *Proc Natl Acad Sci U S A*. 1997;94(24):12863-12868.

49. Prigent C, Satoh MS, Daly G, Barnes DE, Lindahl T. Aberrant DNA repair and DNA replication due to an inherited enzymatic defect in human DNA ligase I. *Mol Cell Biol*. 1994;14(1):310-317.

50. Bentley DJ, Selfridge J, Millar JK, et al. DNA ligase I is required for fetal liver erythropoiesis but is not essential for mammalian cell viability. *Nat Genet*. 1996;13(4):489-491.

51. Barnes DE, Tomkinson AE, Lehmann AR, Webster ADB, Lindahl T. Mutations in the DNA ligase I gene of an individual with immunodeficiencies and cellular hypersensitivity to DNA-damaging agents. *Cell*. 1992;69(3):495-503.

52. Prigent C, Satoh MS, Daly G, Barnes DE, Lindahl T. Aberrant DNA repair and DNA replication due to an inherited enzymatic defect in human DNA ligase I. *Mol Cell Biol*. 1994;14(1):310-317.

53. Hsieh CL, Arlett CF, Lieber MR. V(D)J recombination in ataxia telangiectasia, bloom's syndrome, and a DNA ligase I-associated immunodeficiency disorder. *J Biol Chem*. 1993;268(27):20105-20109.

54. Harrison C, Ketchen AM, Redhead NJ, O'Sullivan MJ, Melton DW. Replication failure, genome instability, and increased cancer susceptibility in mice with a point mutation in the DNA ligase I gene. *Cancer Res*. 2002;62(14):4065-4074.

55. Lakshmipathy U, Campbell C. The human DNA ligase III gene encodes nuclear and mitochondrial proteins. *Mol Cell Biol*. 1999;19(5):3869-3876.

56. Mackey ZB, Ramos W, Levin DS, Walter CA, McCarrey JR, Tomkinson AE. An alternative splicing event which occurs in mouse pachytene spermatocytes generates a form of DNA ligase III with distinct biochemical properties that may function in meiotic recombination. *Mol Cell Biol*. 1997;17(2):989-998.

57. Dong Z, Tomkinson AE. ATM mediates oxidative stress-induced dephosphorylation of DNA ligase IIIalpha. *Nucleic Acids Res*. 2006;34(20):5721-5279.

58. Simsek D, Furda A, Gao Y, et al. Crucial role for DNA ligase III in mitochondria but not in Xrcc1-dependent repair. *Nature*. 2011;471(7337):245-248.

59. Caldecott KW, McKeown CK, Tucker JD, Ljungquist S, Thompson LH. An interaction between the mammalian DNA repair protein XRCC1 and DNA ligase III. *Mol Cell Biol*. 1994;14(1):68-76.

60. Wei YF, Robins P, Carter K, et al. Molecular cloning and expression of human cDNAs encoding a novel DNA ligase IV and DNA

ligase III, an enzyme active in DNA repair and recombination. *Mol Cell Biol*. 1995;15(6):3206-3216.

61. Bryans M, Valenzano MC, Stamato TD. Absence of DNA ligase IV protein in XR-1 cells: Evidence for stabilization by XRCC4. *Mutat Res /DNA Repair*. 1999;433(1):53-58.

62. Chistiakov DA, Voronova NV, Chistiakov AP. Ligase IV syndrome. *European journal of medical genetics*. 2009;52(6):373-378.

63. Rucci F, Notarangelo LD, Fazeli A, et al. Homozygous DNA ligase IV R278H mutation in mice leads to leaky SCID and represents a model for human LIG4 syndrome. *Proc Natl Acad Sci U S A*. 2010;107(7):3024-3029.

64. Grawunder U, Zimmer D, Fugmann S, Schwarz K, Lieber MR. DNA ligase IV is essential for V (D) J recombination and DNA double-strand break repair in human precursor lymphocytes. *Mol Cell*. 1998;2(4):477-484.

65. Frank KM, Sekiguchi JM, Seidl KJ, et al. Late embryonic lethality and impaired V (D) J recombination in mice lacking DNA ligase IV. *Nature*. 1998;396(6707):173-177.

66. Levine AJ. p53, the cellular gatekeeper for growth and division. *Cell*. 1997;88(3):323-331.

67. Lieber MR. The mechanism of double-strand DNA break repair by the nonhomologous DNA end-joining pathway. *Annu Rev Biochem*. 2010;79:181-211.

68. Lieber MR, Ma Y, Pannicke U, Schwarz K. The mechanism of vertebrate nonhomologous DNA end joining and its role in V (D) J recombination. *DNA repair*. 2004;3(8):817-826.

69. Takata M, Sasaki MS, Sonoda E, et al. Homologous recombination and non-homologous end-joining pathways of DNA double-strand break repair have overlapping roles in the maintenance of chromosomal integrity in vertebrate cells. *EMBO J*. 1998;17(18):5497-5508.

70. Roth D, Wilson J. Illegitimate recombination in mammalian cells. *Genetic recombination.American Society for Microbiology, Washington, DC*. 1988:621-653.

71. Downs JA, Jackson SP. A means to a DNA end: The many roles of ku. *Nature Reviews Molecular Cell Biology*. 2004;5(5):367-378.

72. Mimori T, Hardin JA. Mechanism of interaction between ku protein and DNA. *J Biol Chem*. 1986;261(22):10375-10379.

73. de Vries E, van Driel W, Bergsma WG, Arnberg AC, van der Vliet, Peter C. HeLa nuclear protein recognizing DNA termini and translocating on DNA forming a regular DNA-multimeric protein complex. *J Mol Biol*. 1989;208(1):65-78.

74. Dynan WS, Yoo S. Interaction of ku protein and DNA-dependent protein kinase catalytic subunit with nucleic acids. *Nucleic Acids Res*. 1998;26(7):1551-1559.

75. Rivera-Calzada A, Spagnolo L, Pearl LH, Llorca O. Structural model of full-length human Ku70–Ku80 heterodimer and its recognition of DNA and DNA-PKcs. *EMBO Rep*. 2007;8(1):56-62.

76. Mahaney BL, Meek K, Lees-Miller SP. Repair of ionizing radiation-induced DNA double-strand breaks by non-homologous end-joining. *Biochem J*. 2009;417(3):639-650.

77. Gu J, Lu H, Tsai AG, Schwarz K, Lieber MR. Single-stranded DNA ligation and XLF-stimulated incompatible DNA end ligation by the XRCC4-DNA ligase IV complex: Influence of terminal DNA sequence. *Nucleic Acids Res*. 2007;35(17):5755-5762.

78. Gu J, Lu H, Tippin B, Shimazaki N, Goodman MF, Lieber MR. XRCC4:DNA ligase IV can ligate incompatible DNA ends and can ligate across gaps. *EMBO J*. 2007;26(4):1010-1023.

79. Leuther KK, Hammarsten O, Kornberg RD, Chu G. Structure of DNA-dependent protein kinase: Implications for its regulation by DNA. *EMBO J*. 1999;18(5):1114-1123.

80. Hammarsten O, Chu G. DNA-dependent protein kinase: DNA binding and activation in the absence of ku. *Proc Natl Acad Sci U S A*. 1998;95(2):525-530.

81. Ma Y, Schwarz K, Lieber MR. The artemis: DNA-PKcs endonuclease cleaves DNA loops, flaps, and gaps. *DNA repair*. 2005;4(7):845-851.

82. Mahaney B, Meek K, Lees-Miller S. Repair of ionizing radiation-induced DNA double-strand breaks by non-homologous end-joining. *Biochem J*. 2009;417:639-650.

83. Moshous D, Callebaut I, de Chasseval R, et al. Artemis, a novel DNA double-strand break repair/V (D) J recombination protein, is mutated in human severe combined immune deficiency. *Cell*. 2001;105(2):177-186.

84. Pannicke U, Ma Y, Hopfner K, Niewolik D, Lieber MR, Schwarz K. Functional and biochemical dissection of the structure-specific nuclease ARTEMIS. *EMBO J*. 2004;23(9):1987-1997.

85. Goodarzi AA, Yu Y, Riballo E, et al. DNA-PK autophosphorylation facilitates artemis endonuclease activity. *EMBO J*. 2006;25(16):3880-3889.

86. De Villartay J, Shimazaki N, Charbonnier J, et al. A histidine in the β-CASP domain of artemis is critical for its full< i> in vitro and< i> in vivo functions. *DNA repair*. 2009;8(2):202-208.

87. Ma Y, Pannicke U, Schwarz K, Lieber MR. Hairpin opening and overhang processing by an artemis/DNA-dependent protein kinase complex in nonhomologous end joining and V (D) J recombination. *Cell*. 2002;108(6):781-794.

88. Li Z, Otevrel T, Gao Y, et al. The XRCC4 gene encodes a novel protein involved in DNA double-strand break repair and V (D) J recombination. *Cell*. 1995;83(7):1079-1089.

89. Modesti M, Junop MS, Ghirlando R, et al. Tetramerization and DNA ligase IV interaction of the DNA double-strand break repair protein XRCC4 are mutually exclusive. *J Mol Biol*. 2003;334(2):215-228.

90. Grawunder U, Wilm M, Wu X, et al. Activity of DNA ligase IV stimulated by complex formation with XRCC4 protein in mammalian cells. *Nature*. 1997;388(6641):492-495.

91. Sibanda BL, Critchlow SE, Begun J, et al. Crystal structure of an Xrcc4–DNA ligase IV complex. *Nature Structural & Molecular Biology*. 2001;8(12):1015-1019.

92. Modesti M, Hesse JE, Gellert M. DNA binding of Xrcc4 protein is associated with V (D) J recombination but not with stimulation of DNA ligase IV activity. *EMBO J*. 1999;18(7):2008-2018.

93. Ahnesorg P, Smith P, Jackson SP. XLF interacts with the XRCC4-DNA ligase IV complex to promote DNA nonhomologous end-joining. *Cell*. 2006;124(2):301-313.

94. Leber R, Wise TW, Mizuta R, Meek K. The XRCC4 gene product is a target for and interacts with the DNA-dependent protein kinase. *J Biol Chem*. 1998;273(3):1794-1801.

95. Nick McElhinny SA, Snowden CM, McCarville J, Ramsden DA. Ku recruits the XRCC4-ligase IV complex to DNA ends. *Mol Cell Biol*. 2000;20(9):2996-3003.

96. Barnes DE, Stamp G, Rosewell I, Denzel A, Lindahl T. Targeted disruption of the gene encoding DNA ligase IV leads to lethality in embryonic mice. *Current Biology*. 1998;8(25):1395-1398.

97. Francis DB, Kozlov M, Chavez J, et al. DNA ligase IV regulates XRCC4 nuclear localization. *DNA repair*. 2014;21:36-42.

98. Buck D, Malivert L, de Chasseval R, et al. Cernunnos, a novel nonhomologous end-joining factor, is mutated in human immunodeficiency with microcephaly. *Cell*. 2006;124(2):287-299.

99. Lange SS, Takata K, Wood RD. DNA polymerases and cancer. *Nature Reviews Cancer*. 2011;11(2):96-110.

100. Bertocci B, De Smet A, Weill J, Reynaud C. Nonoverlapping functions of DNA polymerases mu, lambda, and terminal deoxynucleotidyltransferase during immunoglobulin V (D) J recombination in vivo. *Immunity*. 2006;25(1):31-41.

101. Mahajan KN, Nick McElhinny SA, Mitchell BS, Ramsden DA. Association of DNA polymerase mu (pol mu) with ku and ligase IV: Role for pol mu in end-joining double-strand break repair. *Mol Cell Biol*. 2002;22(14):5194-5202.

102. Garcia-Diaz M, Bebenek K, Larrea AA, et al. Template strand scrunching during DNA gap repair synthesis by human polymerase λ. *Nature structural & molecular biology*. 2009;16(9):967-972.

103. Lucas D, Escudero B, Ligos JM, et al. Altered hematopoiesis in mice lacking DNA polymerase μ is due to inefficient double-strand break repair. *PLoS genetics*. 2009;5(2):e1000389.

104. DeFazio LG, Stansel RM, Griffith JD, Chu G. Synapsis of DNA ends by DNA-dependent protein kinase. *EMBO J*. 2002;21(12):3192-3200.

105. Someya M, Sakata K, Matsumoto Y, et al. The association of DNA-dependent protein kinase activity with chromosomal instability and risk of cancer. *Carcinogenesis*. 2006;27(1):117-122.

106. Hatanpaa KJ, Burma S, Zhao D, Habib AA. Epidermal growth factor receptor in glioma: Signal transduction, neuropathology, imaging, and radioresistance. *Neoplasia*. 2010;12(9):675-684.

107. Begg AC, Stewart FA, Vens C. Strategies to improve radiotherapy with targeted drugs. *Nature Reviews Cancer*. 2011;11(4):239-253.

108. Beskow C, Skikuniene J, Holgersson Å, et al. Radioresistant cervical cancer shows upregulation of the NHEJ proteins DNA-PKcs, Ku70 and Ku86. *Br J Cancer*. 2009;101(5):816-821.

109. Pucci S, Mazzarelli P, Rabitti C, et al. Tumor specific modulation of KU70/80 DNA binding activity in breast and bladder human tumor biopsies. *Oncogene*. 2001;20(6):739-747.

110. Parrella P, Mazzarelli P, Signori E, et al. Expression and heterodimer-binding activity of Ku70 and Ku80 in human non-melanoma skin cancer. *J Clin Pathol*. 2006;59(11):1181-1185.

111. Shintani S, Mihara M, Li C, et al. Up-regulation of DNA-dependent protein kinase correlates with radiation resistance in oral squamous cell carcinoma. *Cancer science*. 2003;94(10):894-900.

112. Hosoi Y, Watanabe T, Nakagawa K, et al. Up-regulation of DNA-dependent protein kinase activity and Sp1 in colorectal cancer. *Int J Oncol*. 2004;25(2):461-468.

113. Chen T, Chen J, Su W, Wu M, Tsao C. Expression of DNA repair gene Ku80 in lymphoid neoplasm. *Eur J Haematol*. 2005;74(6):481-488.

114. Kuschel B, Auranen A, McBride S, et al. Variants in DNA double-strand break repair genes and breast cancer susceptibility. *Hum Mol Genet*. 2002;11(12):1399-1407.

115. Holgersson Å, Nilsson A, Lewensohn R, Kanter L. Expression of DNA-PKcs and Ku86, but not Ku70, differs between lymphoid malignancies. *Exp Mol Pathol*. 2004;77(1):1-6.

116. Muller C, Christodoulopoulos G, Salles B, Panasci L. DNA-dependent protein kinase activity correlates with clinical and in vitro sensitivity of chronic lymphocytic leukemia lymphocytes to nitrogen mustards. *Blood*. 1998;92(7):2213-2219.

117. Elliott SL, Crawford C, Mulligan E, et al. Mitoxantrone in combination with an inhibitor of DNA-dependent protein kinase: A potential therapy for high risk b-cell chronic lymphocytic leukaemia. *Br J Haematol*. 2011;152(1):61-71.

118. Srivastava M, Raghavan SC. DNA double-strand break repair inhibitors as cancer therapeutics. *Chem Biol*. 2015;22(1):17-29.

119. Sarkaria JN, Tibbetts RS, Busby EC, Kennedy AP, Hill DE, Abraham RT. Inhibition of phosphoinositide 3-kinase related kinases by the radiosensitizing agent wortmannin. *Cancer Res*. 1998;58(19):4375-4382.

120. Chernikova S, Wells R, Elkind M. Wortmannin sensitizes mammalian cells to radiation by inhibiting the DNA-dependent protein kinase-mediated rejoining of double-strand breaks. *Radiat Res*. 1999;151(2):159-166.

121. Rosenzweig KE, Youmell MB, Palayoor ST, Price BD. Radiosensitization of human tumor cells by the phosphatidylinositol3-kinase inhibitors wortmannin and LY294002 correlates with inhibition of DNA-dependent protein kinase and prolonged G2-M delay. *Clin Cancer Res*. 1997;3(7):1149-1156.

122. Veuger SJ, Curtin NJ, Richardson CJ, Smith GC, Durkacz BW. Radiosensitization and DNA repair inhibition by the combined use of novel inhibitors of DNA-dependent protein kinase and poly(ADP-ribose) polymerase-1. *Cancer Res*. 2003;63(18):6008-6015.

123. Chen X, Zhong S, Zhu X, et al. Rational design of human DNA ligase inhibitors that target cellular DNA replication and repair. *Cancer Res*. 2008;68(9):3169-3177.

124. Srivastava M, Nambiar M, Sharma S, et al. An inhibitor of nonhomologous end-joining abrogates double-strand break repair and impedes cancer progression. *Cell*. 2012;151(7):1474-1487.

125. Rai KR, Sawitsky A, Cronkite EP, Chanana AD, Levy RN, Pasternack BS. Clinical staging of chronic lymphocytic leukemia. *Blood*. 1975;46(2):219-234.

126. Küppers R. Mechanisms of B-cell lymphoma pathogenesis. *Nature Reviews Cancer*. 2005;5(4):251-262.

127. Fais F, Ghiotto F, Hashimoto S, et al. Chronic lymphocytic leukemia B cells express restricted sets of mutated and unmutated antigen receptors. *J Clin Invest*. 1998;102(8):1515-1525.

128. Zenz T, Mertens D, Küppers R, Döhner H, Stilgenbauer S. From pathogenesis to treatment of chronic lymphocytic leukaemia. *Nature Reviews Cancer*. 2010;10(1):37-50.

129. Binet J, Leporrier M, Dighiero G. A clinical staging system for chronic lymphocytic leukemia: Prognostic signi? cance. *Cancer*. 1977;40.

130. Rai KR, Sawitsky A, Cronkite EP, Chanana AD, Levy RN, Pasternack BS. Clinical staging of chronic lymphocytic leukemia. *Blood*. 1975;46(2):219-234.

131. Nabhan C, Rosen ST. Chronic lymphocytic leukemia: A clinical review. *JAMA*. 2014;312(21):2265-2276.

132. Zhu Q, Tan D, Samuel M, Chan E, Linn Y. Fludarabine in comparison to alkylator-based regimen as induction therapy for chronic lymphocytic leukemia: A systematic review and meta-analysis. *Leuk Lymphoma*. 2004;45(11):2239-2245.

133. Byrd JC, Peterson BL, Morrison VA, et al. Randomized phase 2 study of fludarabine with concurrent versus sequential treatment with rituximab in symptomatic, untreated patients with B-cell chronic lymphocytic leukemia: Results from cancer and leukemia group B 9712 (CALGB 9712). *Blood*. 2003;101(1):6-14.

134. Shatnyeva OM, Hansen HP, Reiners KS, Sauer M, Vyas M, von Strandmann EP. DNA damage response and evasion from immunosurveillance in CLL: New options for NK cell-based immunotherapies. *Front Genet*. 2015;6:11.

135. Reinhardt HC, Yaffe MB. Kinases that control the cell cycle in response to DNA damage: Chk1, Chk2, and MK2. *Curr Opin Cell Biol*. 2009;21(2):245-255.

136. Schwarz JK, Lovly CM, Piwnica-Worms H. Regulation of the Chk2 protein kinase by oligomerization-mediated cis- and trans-phosphorylation. *Mol Cancer Res*. 2003;1(8):598-609.

137. Zhao H, Piwnica-Worms H. ATR-mediated checkpoint pathways regulate phosphorylation and activation of human Chk1. *Mol Cell Biol*. 2001;21(13):4129-4139.

138. Donzelli M, Draetta GF. Regulating mammalian checkpoints through Cdc25 inactivation. *EMBO Rep*. 2003;4(7):671-677.

139. Bartkova J, Hořejší Z, Koed K, et al. DNA damage response as a candidate anti-cancer barrier in early human tumorigenesis. *Nature*. 2005;434(7035):864-870.

140. Austen B, Skowronska A, Baker C, et al. Mutation status of the residual ATM allele is an important determinant of the cellular response to chemotherapy and survival in patients with chronic lymphocytic leukemia containing an 11q deletion. *J Clin Oncol*. 2007;25(34):5448-5457.

141. Shiloh Y, Ziv Y. The ATM protein kinase: Regulating the cellular response to genotoxic stress, and more. *Nature reviews Molecular cell biology*. 2013;14(4):197-210.

142. Burger JA, Gribben JG. The microenvironment in chronic lymphocytic leukemia (CLL) and other B cell malignancies: Insight into disease biology and new targeted therapies. . 2014;24:71-81.

143. Rangwala S, Zhang C, Duvic M. HDAC inhibitors for the treatment of cutaneous T-cell lymphomas. *Future medicinal chemistry*. 2012;4(4):471-486.

144. Smith S, Fox J, Mejia M, et al. Histone deacetylase inhibitors selectively target homology dependent DNA repair defective cells and elevate non-homologous endjoining activity. *PloS one*. 2014;9(1).

145. Henrich S, Christopherson R. Multiple forms of nuclear p53 formed in human raji and MEC1 cells treated with fludarabine. *Leukemia*. 2008;22(3):657-660.

146. Fei P, El-Deiry WS. P53 and radiation responses. *Oncogene*. 2003;22(37):5774-5783.

147. Sun D, Urrabaz R, Nguyen M, et al. Elevated expression of DNA ligase I in human cancers. *Clin Cancer Res*. 2001;7(12):4143-4148.

148. Sallmyr A, Tomkinson AE, Rassool FV. Up-regulation of WRN and DNA ligase IIIalpha in chronic myeloid leukemia: Consequences for the repair of DNA double-strand breaks. *Blood*. 2008;112(4):1413-1423.

149. Riballo E, Critchlow S, Teo S, et al. Identification of a defect in DNA ligase IV in a radiosensitive leukaemia patient. *Current biology*. 1999;9(13):699-S2.

150. Kuhmann C, Li C, Kloor M, et al. Altered regulation of DNA ligase IV activity by aberrant promoter DNA methylation and gene amplification in colorectal cancer. *Hum Mol Genet*. 2014;23(8):2043-2054.

151. Ben-Omran TI, Cerosaletti K, Concannon P, Weitzman S, Nezarati MM. A patient with mutations in DNA ligase IV: Clinical features and overlap with nijmegen breakage syndrome. *American Journal of Medical Genetics Part A*. 2005;137(3):283-287.

152. Fox JT, Sakamuru S, Huang R, et al. High-throughput genotoxicity assay identifies antioxidants as inducers of DNA damage response and cell death. *Proc Natl Acad Sci U S A*. 2012;109(14):5423-5428.

153. Dokmanovic M, Clarke C, Marks PA. Histone deacetylase inhibitors: Overview and perspectives. *Mol Cancer Res*. 2007;5(10):981-989.

154. Lomax M, Folkes L, O'Neill P. Biological consequences of radiation-induced DNA damage: Relevance to radiotherapy. *Clin Oncol*. 2013;25(10):578-585.

155. Rothkamm K, Lobrich M. Evidence for a lack of DNA double-strand break repair in human cells exposed to very low x-ray doses. *Proc Natl Acad Sci U S A*. 2003;100(9):5057-5062.

156. Sleiman RJ, Stewart BW. Early caspase activation in leukemic cells subject to etoposide-induced G2-M arrest: Evidence of commitment to apoptosis rather than mitotic cell death. *Clin Cancer Res*. 2000;6(9):3756-3765.

157. Gottlieb TM, Oren M. p53 in growth control and neoplasia. *Biochimica et Biophysica Acta (BBA)-Reviews on Cancer*. 1996;1287(2):77-102.

158. Hollstein M, Sidransky D, Vogelstein B, Harris CC. P53 mutations in human cancers. *Science*. 1991;253(5015):49-53.

159. Carlomagno F, Burnet NG, Turesson I, et al. Comparison of DNA repair protein expression and activities between human fibroblast cell lines with different radiosensitivities. *International journal of cancer*. 2000;85(6):845-849.